The Abdus Salam
International Centre for Theoretical Physics

United Nations
Educational, Scientific and
Cultural Organization

IAEA
International Atomic Energy Agency

2066-1

Workshop and Conference on Biogeochemical Impacts of Climate and Land-Use Changes on Marine Ecosystems

2 - 10 November 2009

Bio-physical interactions: from basin to submesoscales

A. Bracco
EAS, Geaorgia Tech
U.S.A.

Bio-physical interactions: from basin to submesoscales

Annalisa Bracco

Georgia Institute of Technology

Earth and Atmospheric Sciences

Tracer conservation and ocean transport

The tracer conservation equation describes

<u>the time rate of change of a tracer at a given point and the processes that change its concentration</u>

The processes include

1. transport and mixing → physical
2. sources and sinks → biological and chemical transformations

The tracer conservation eq. for a volume at a fxed location is

$$\frac{\partial C}{\partial t} = \left.\frac{\partial C}{\partial t}\right|_{advection} + \left.\frac{\partial C}{\partial t}\right|_{diffusion} + SMS(C)$$

where SMS(C) (mmol m^{-3} s^{-1}) represents internal sources minus sinks

Advection

The large-scale, depth integrated ocean circulation:

- The wind-drive gyre circulation and the Stommel model
- The Meridional Overturning Circulation

The wind-driven circulation

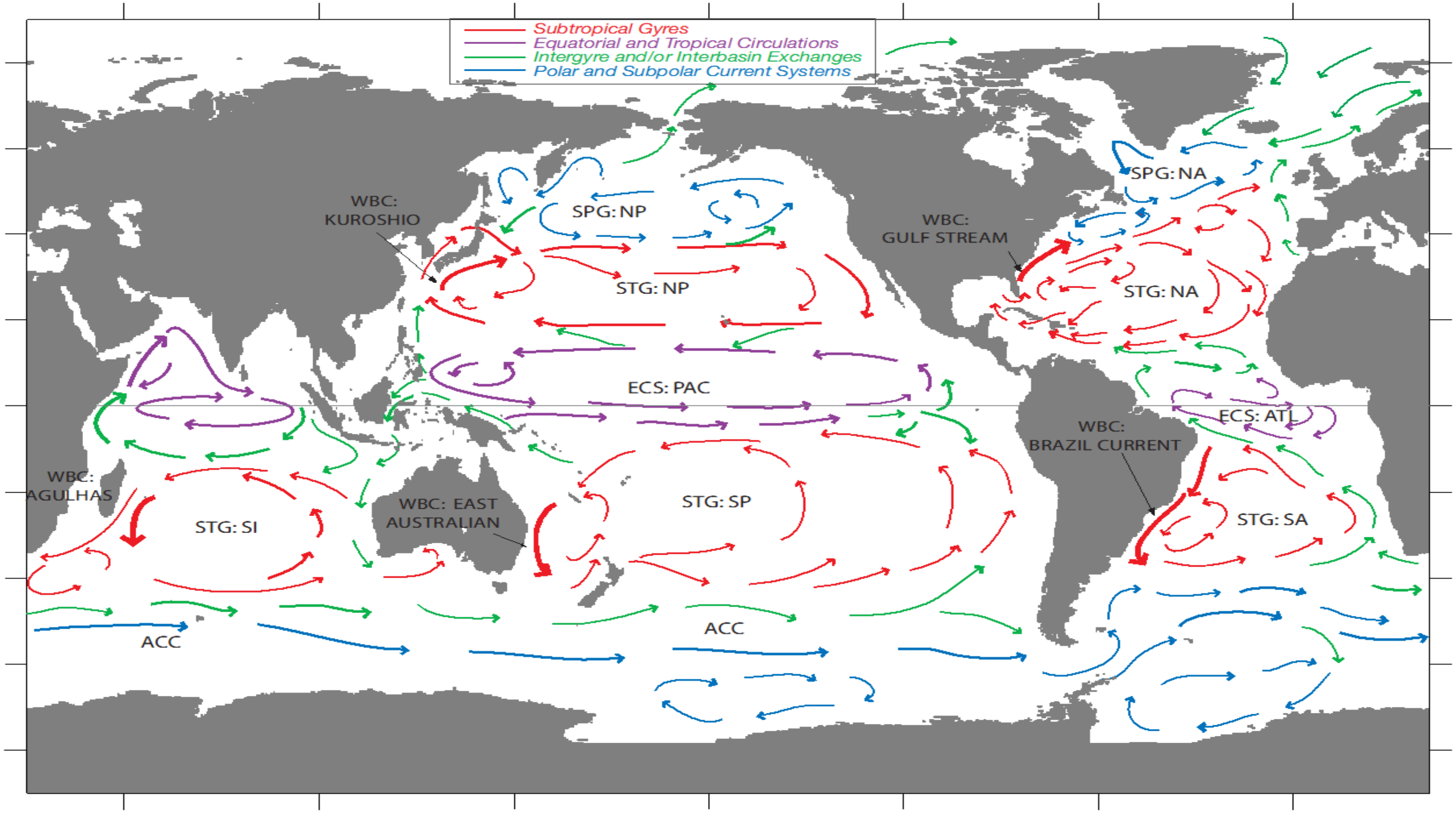

Fig. 14.1 A schema of the main currents of the global ocean. Key: STG – Sub-Tropical Gyre; SPG – Sub-Polar Gyre; WBC – Western Boundary Current; ECS – Equatorial Current System; NA – North Atlantic; SA – South Atlantic; NP – North Pacific; SP – South Pacific; SI – South Indian; ACC – Antarctic Circumpolar Current; ATL – Atlantic; PAC – Pacific.

- The large-scale circulation is given by subpolar (cyclonic) and subtropical gyres (anticyclonic)
- Exception at the equator → surface currents are predominantly westwards and the vertical integrated flow is eastward
- The gyres are strongest in the west → intensification of western boundary currents
- Western boundary currents from subpolar and subtropical gyres lead to the Gulf Stream, Kuroshio and Brazilian currents

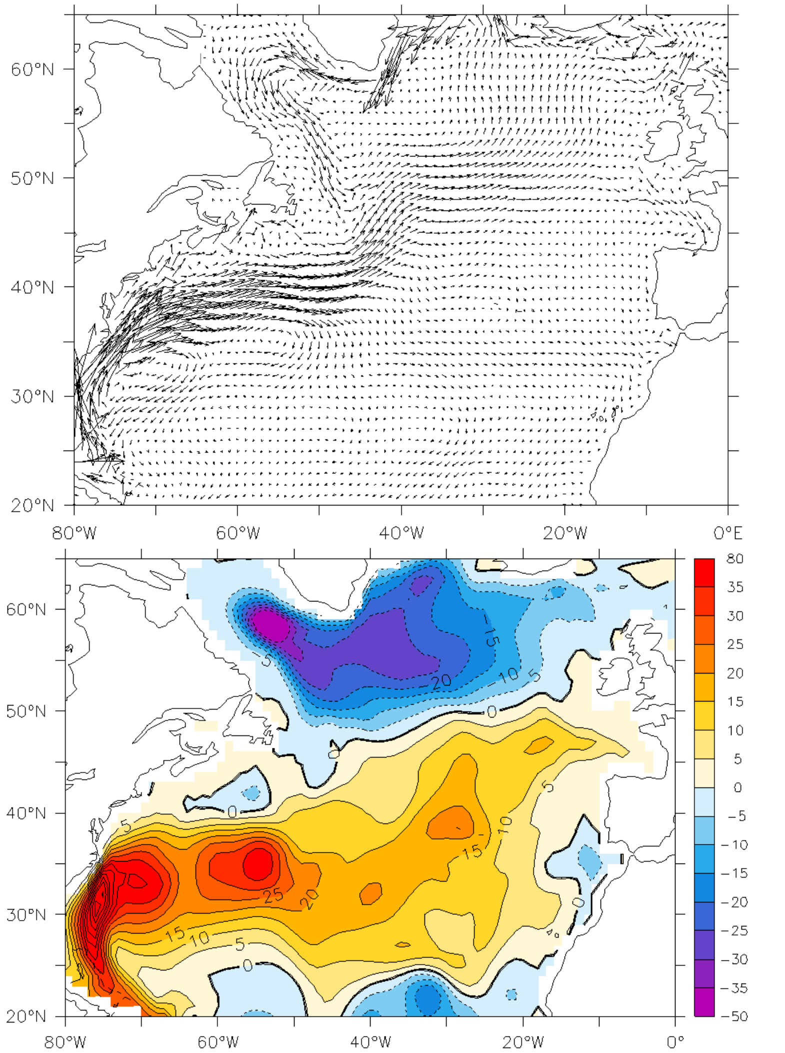

Fig. 14.2 Top: The time-averaged velocity field at a depth of 75 m in the North Atlantic, obtained by constraining a numerical model to hydrographic observations. Bottom: The streamfunction of the vertically integrated flow, in Sverdrups. Note the presence of an anticyclonic subtropical gyre, a cyclonic subpolar gyre, and intense western boundary currents.[3]

The zero-order features of the ocean gyre circulation has been described by a steady, forced-dissipative, homogeneous model proposed by Stommel (1948)

The Stommel model

The planetary geostrophic eq. for a Boussinesq fluid in the limit of small Rossby number are:

$$\frac{Db}{Dt} = \dot{b}$$

thermodynamic eq

$$\nabla \cdot \vec{v} = 0$$

continuity

$$\vec{f} \times \vec{u} = -\nabla \phi + \frac{1}{\rho_o} \frac{\partial \vec{\tau}}{\partial z}$$

horizontal momentum
(geostrophic balance + wind stress)

$$\frac{\partial \phi}{\partial z} = b$$

vertical momentum
(geostrophic balance)

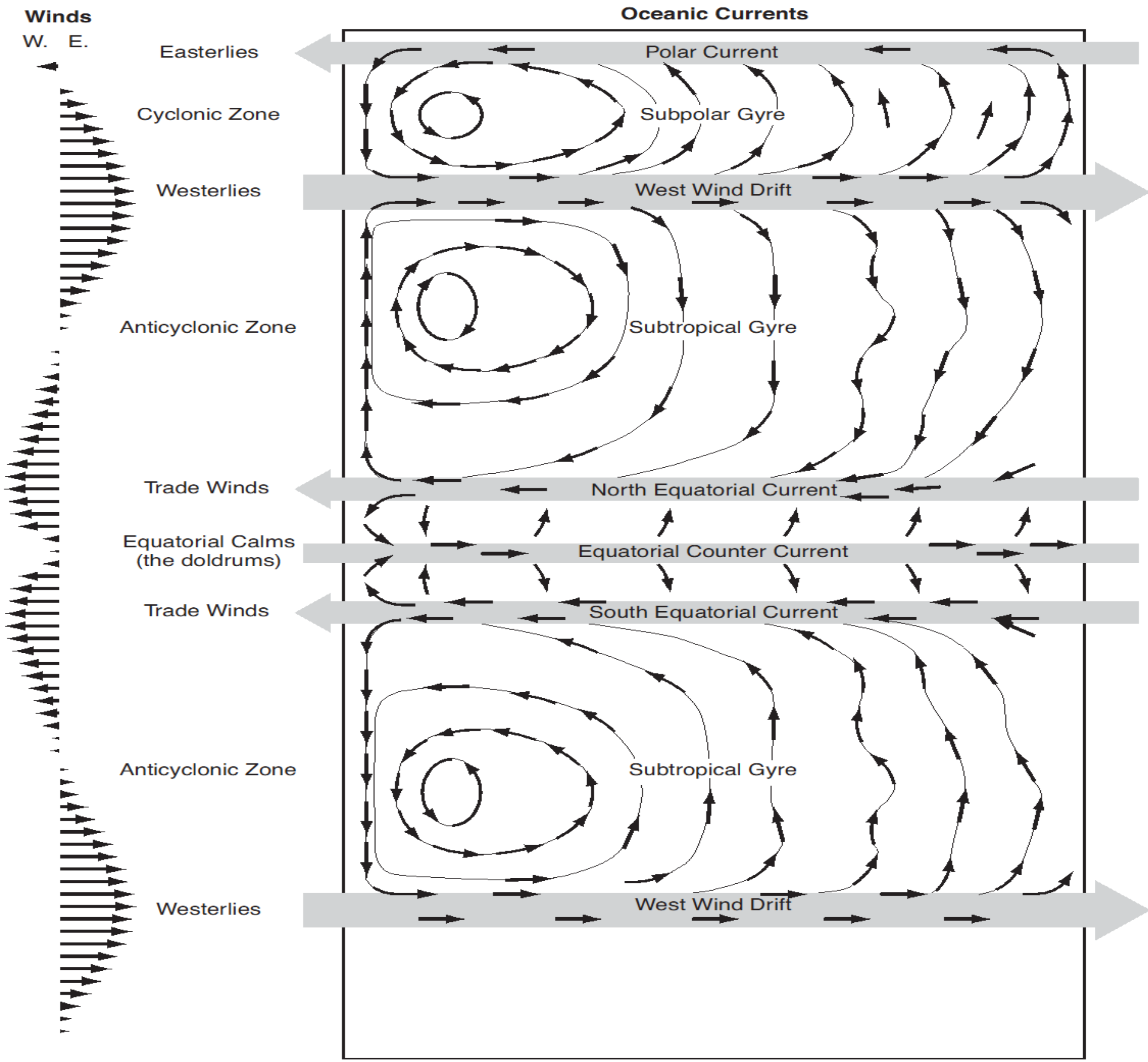

Winds
W. E.
Oceanic Currents
Easterlies
Polar Current
Cyclonic Zone
Subpolar Gyre
Westerlies
West Wind Drift
Anticyclonic Zone
Subtropical Gyre
Trade Winds
North Equatorial Current
Equatorial Calms (the doldrums)
Equatorial Counter Current
Trade Winds
South Equatorial Current
Anticyclonic Zone
Subtropical Gyre
Westerlies
West Wind Drift

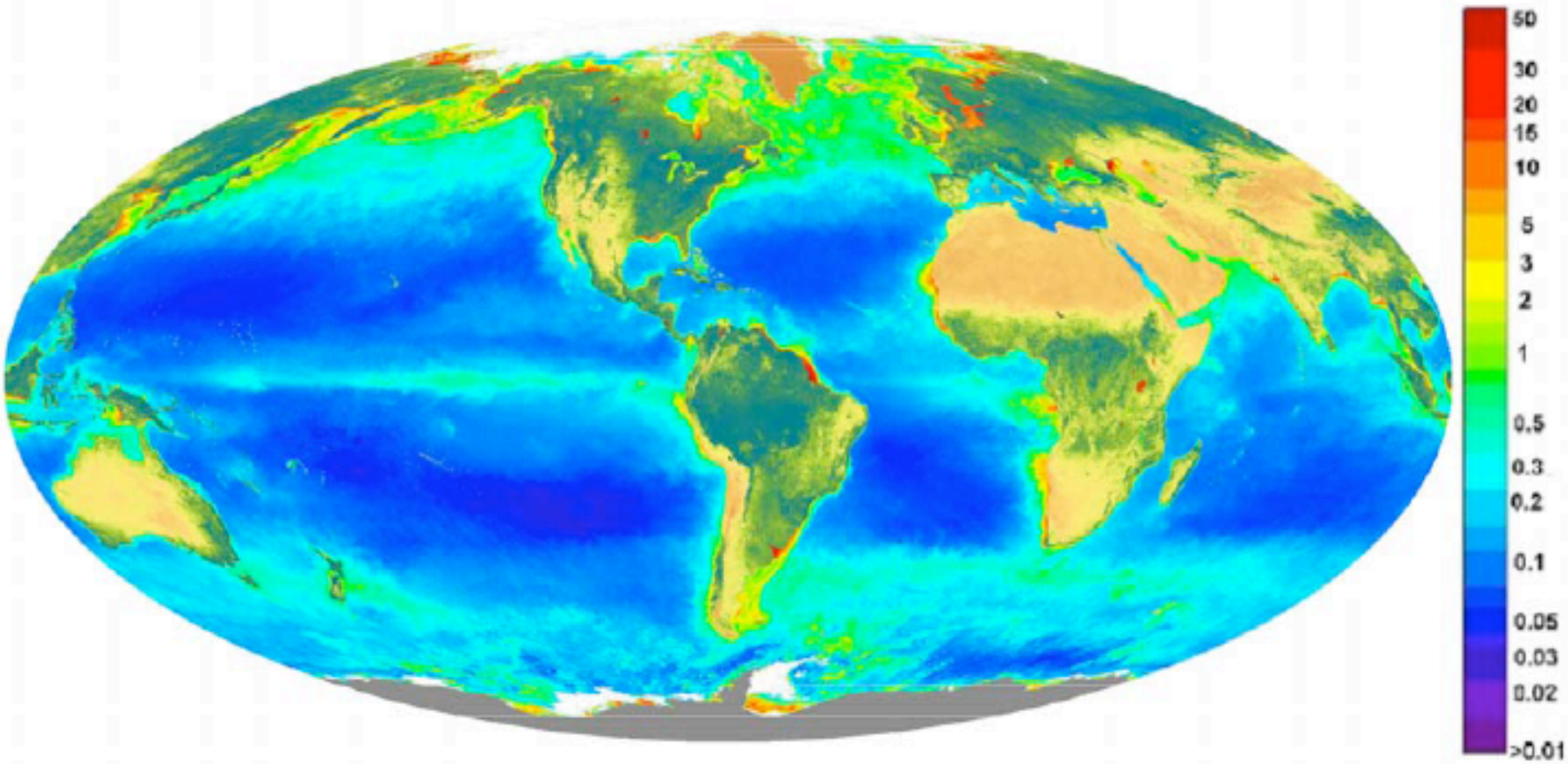

Figure 2: Estimate of phytoplankton distribution in the surface ocean: global composite image of surface chlorophyll a concentration (mg m^{-3}) estimated from SeaWiFS data (Source: NASA Goddard Space Flight Center, Maryland, USA and ORBIMAGE, Virginia, USA).

Upwelling and downwelling associated to the Ekman transport

cyclonic circulation

anticyclonic circulation

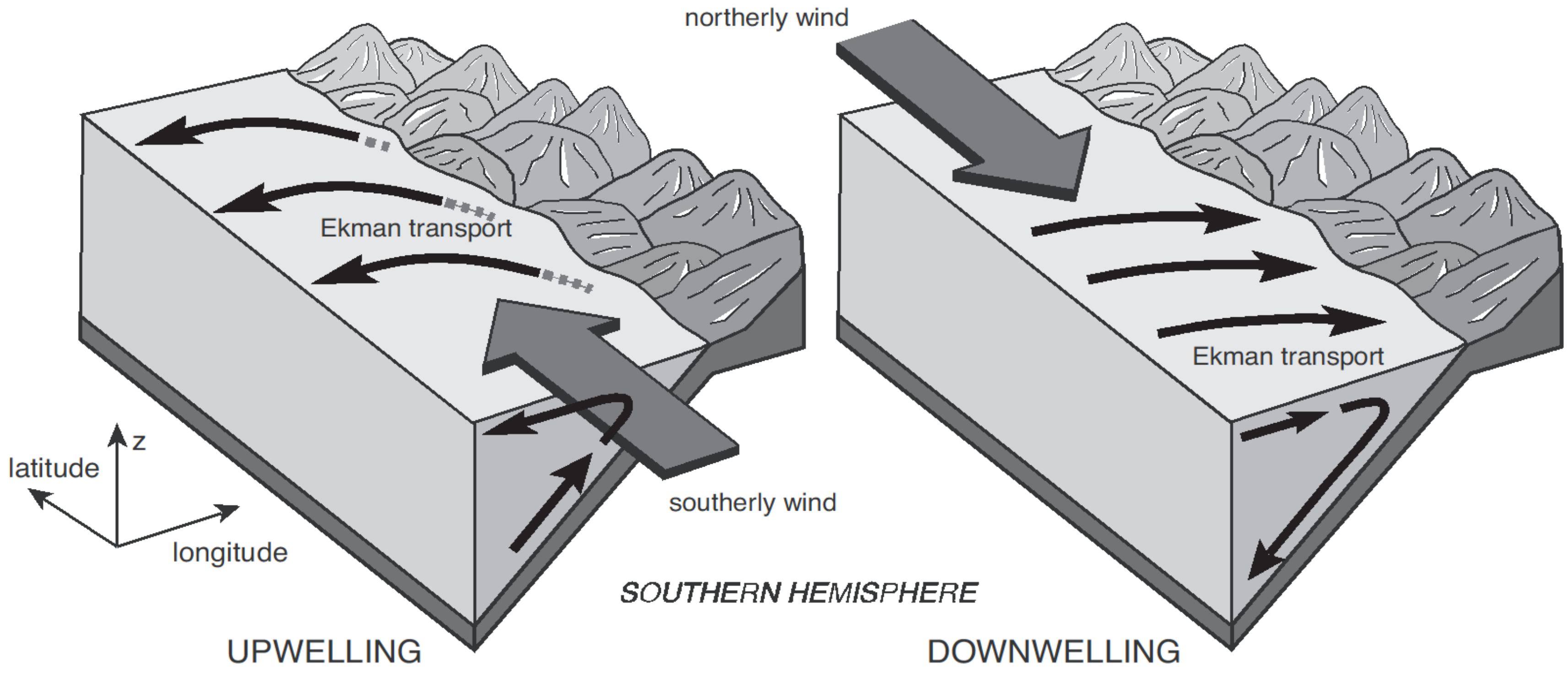

and to equatorial divergence and subtropical convergence

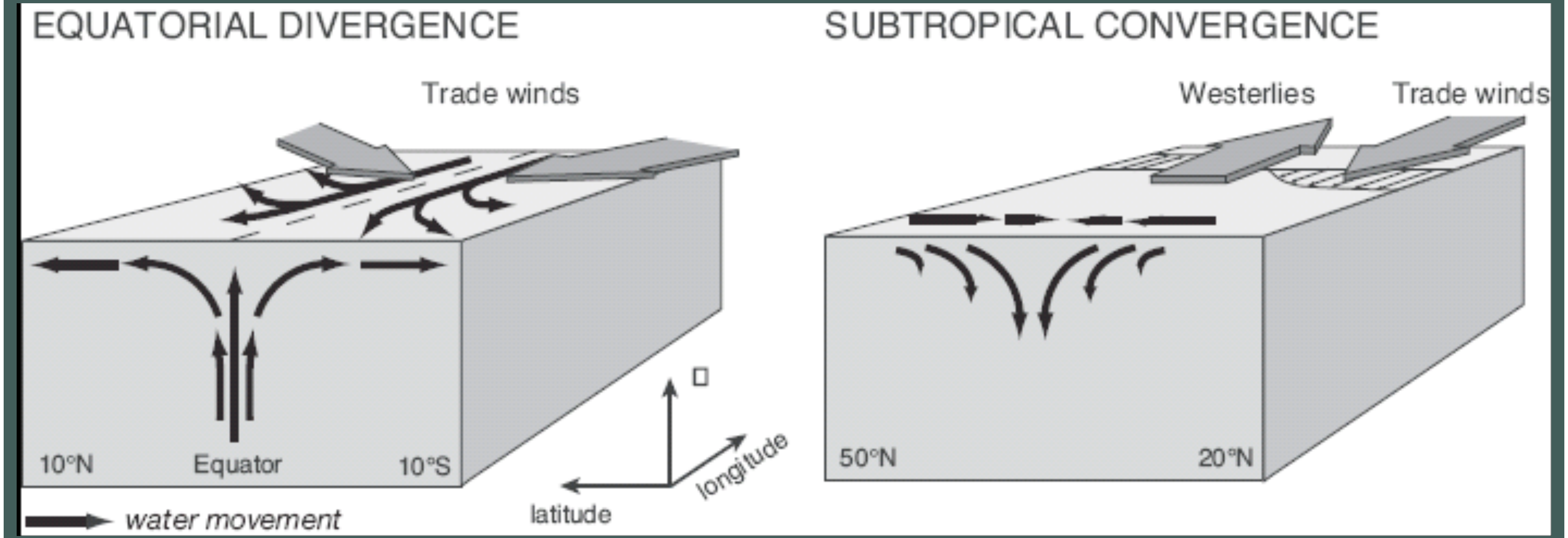

averaged vertical velocities

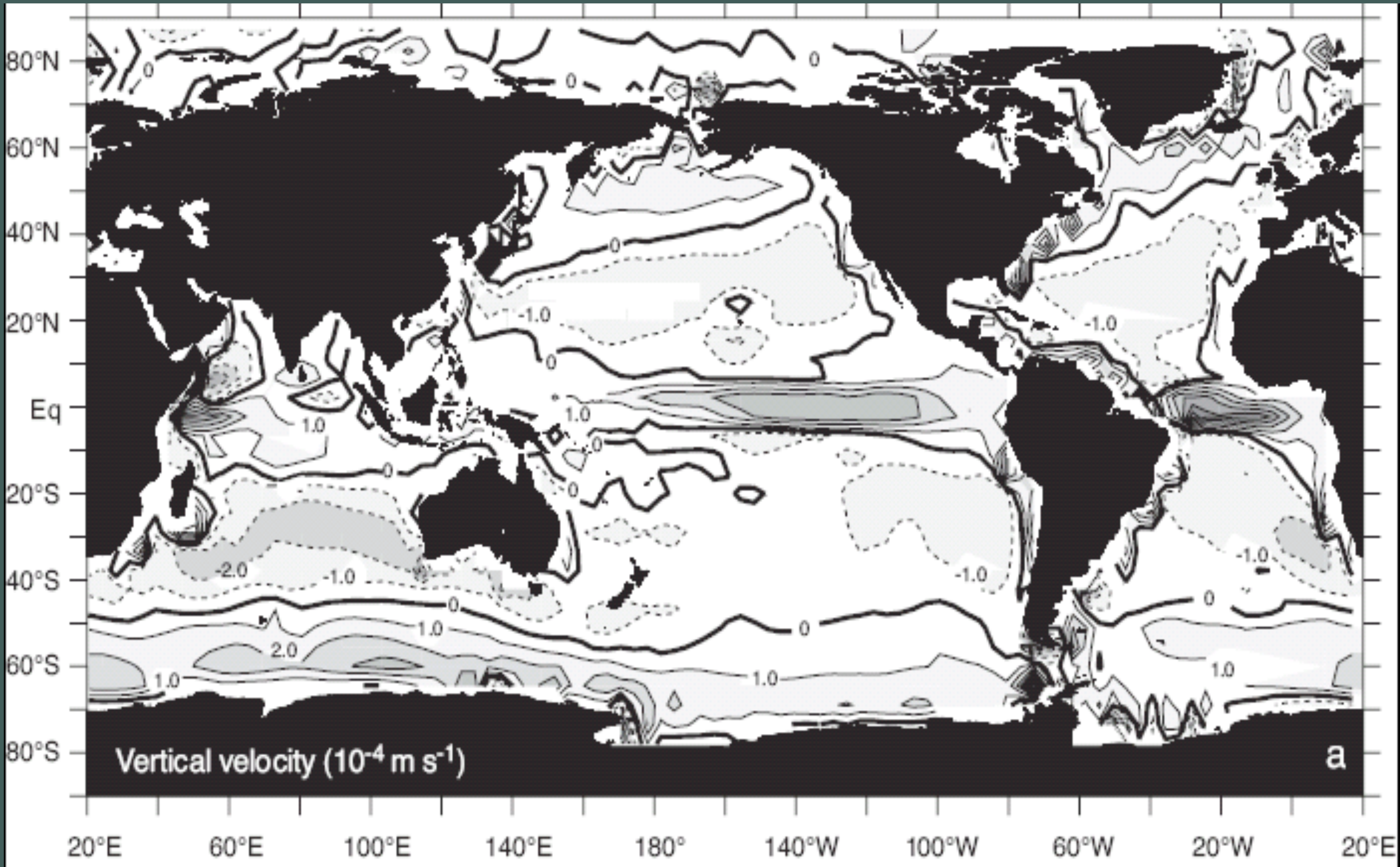

impact on biogeochemistry: production associated with the vertical velocities in the gyres

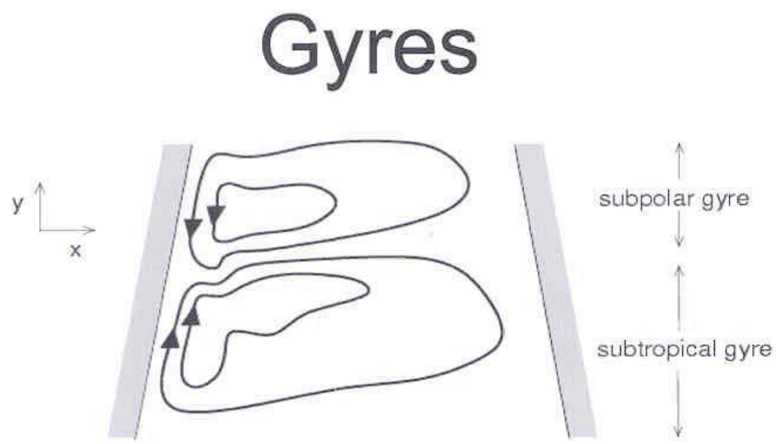

from Williams and Follows, 1998

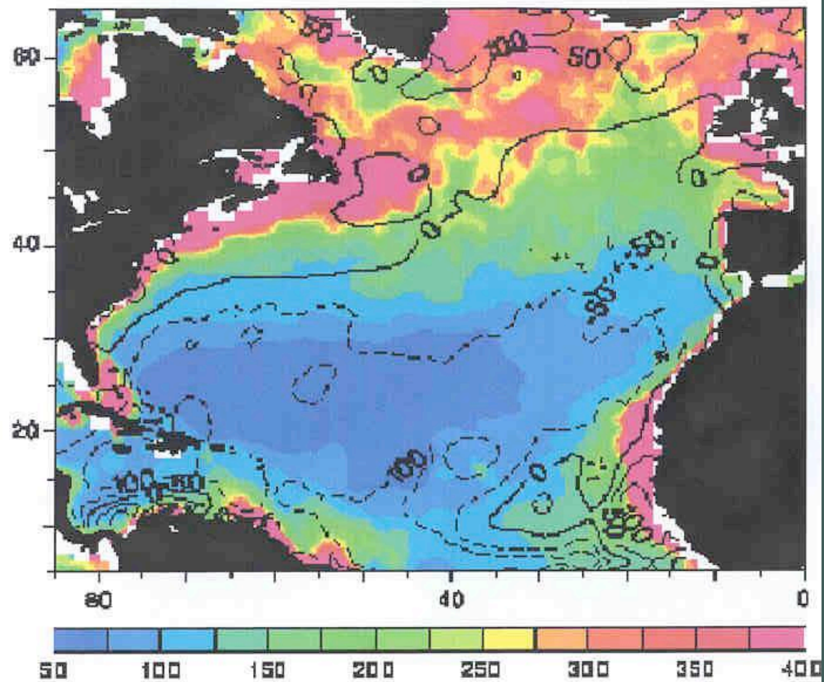

w (m y^{-1}) (contours)
Export production
(gC m^{-2} y^{-1}) (colour)

impact on biogeochemistry: production associated with the horizontal velocities

Lateral transfer of nitrate

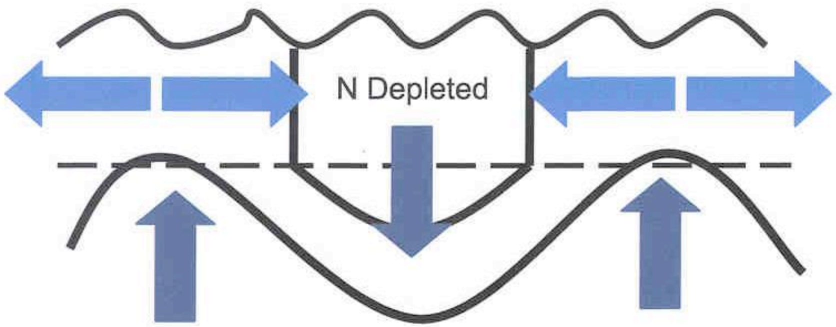

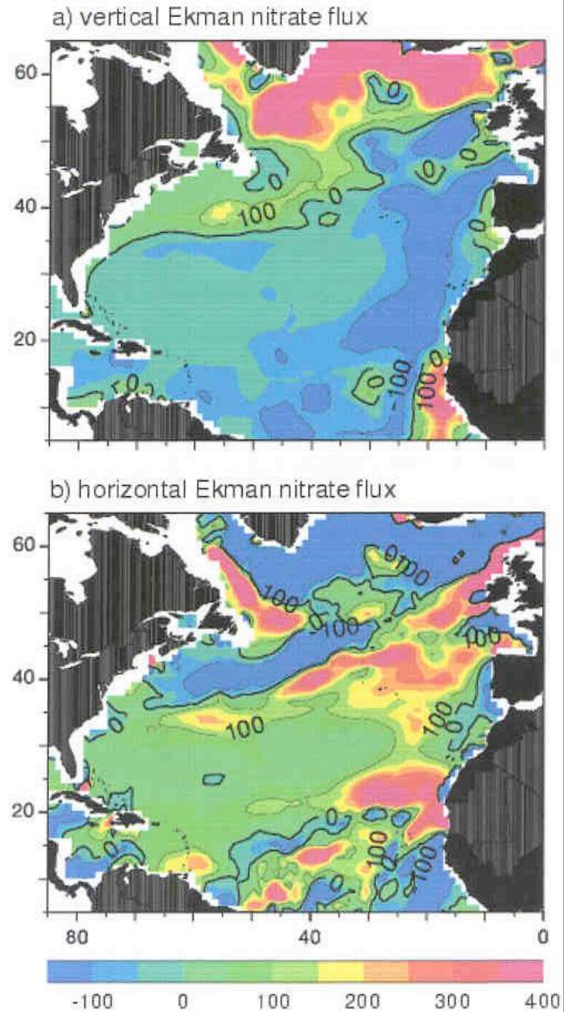

Williams & Follows(1998)

What about the vertical distributions?

The MOC (or thermohaline circulation)

- The meridional overturning circulation is responsible for the abyssal circulation in the ocean.
- It is also called thermohaline circulation because is driven principally by temperature and salinity
- A satisfactory theory explaining the MOC is not available. Simple models lack important components and are not as accurate as the one describing the wind-driven circulation

The MOC

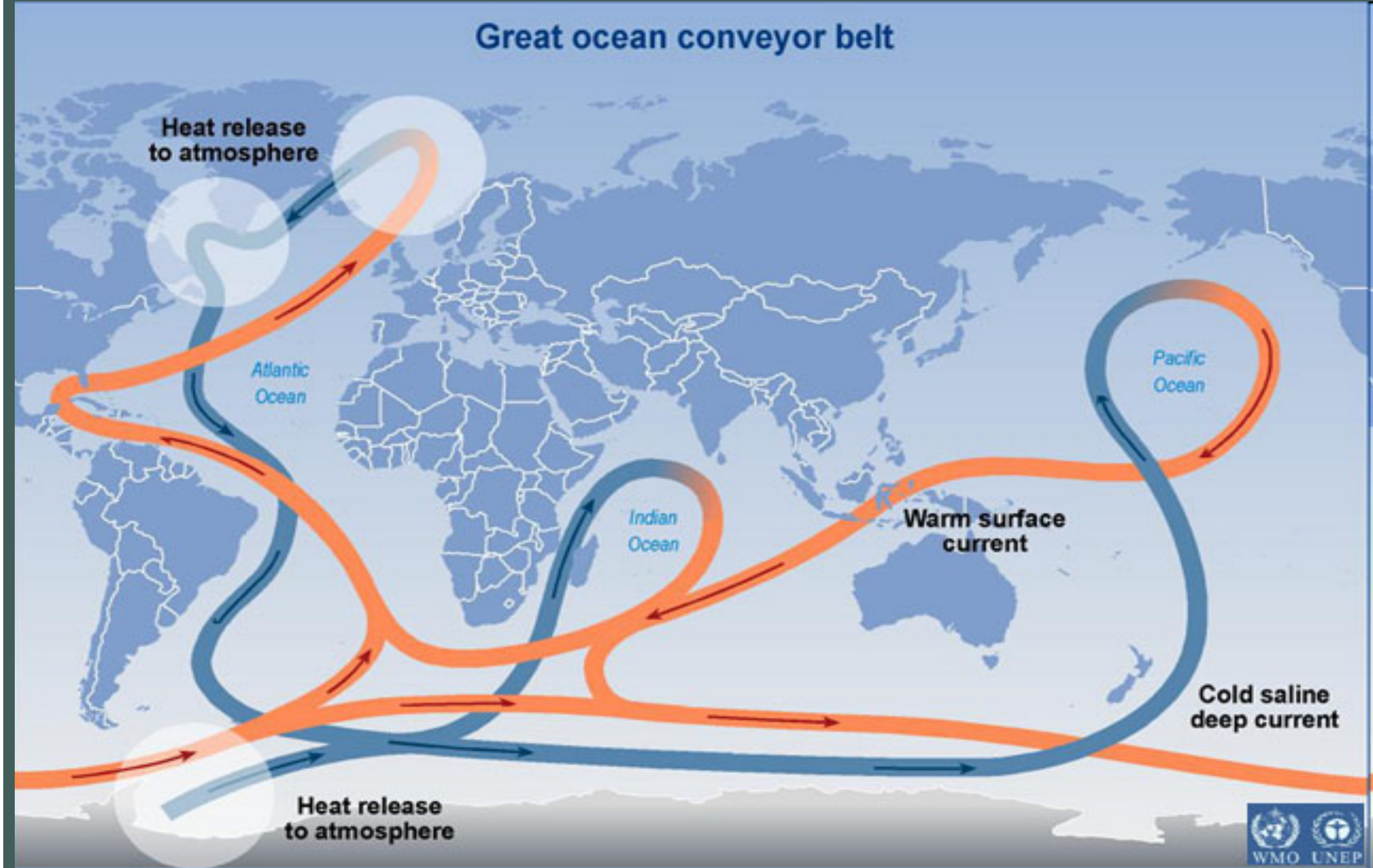
Great ocean conveyor belt
Heat release
to atmosphere
Atlantic
Ocean
Indian
Ocean
Pacific
Ocean
Warm surface
current
Cold saline
deep current
Heat release
to atmosphere
WMO UNEP

Associated with the MOC there is a distinctive stratification.

- Most of stratification is concentrated in the first upper kilometer
- The relatively unstratified abyss water originates at high latitudes (with outcropping only in the North Atlantic subpolar gyre and in the Antarctic Circumpolar Current - ACC)

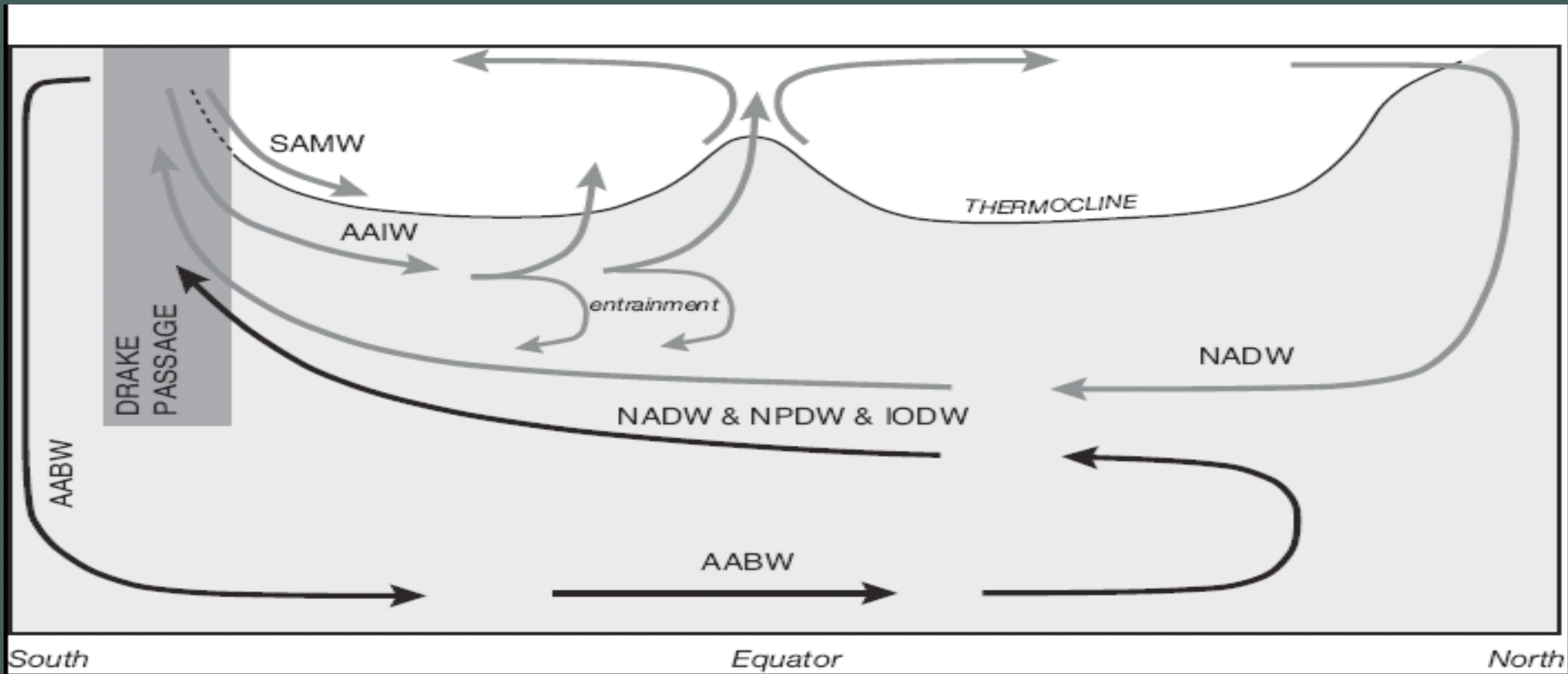

Potential temperature

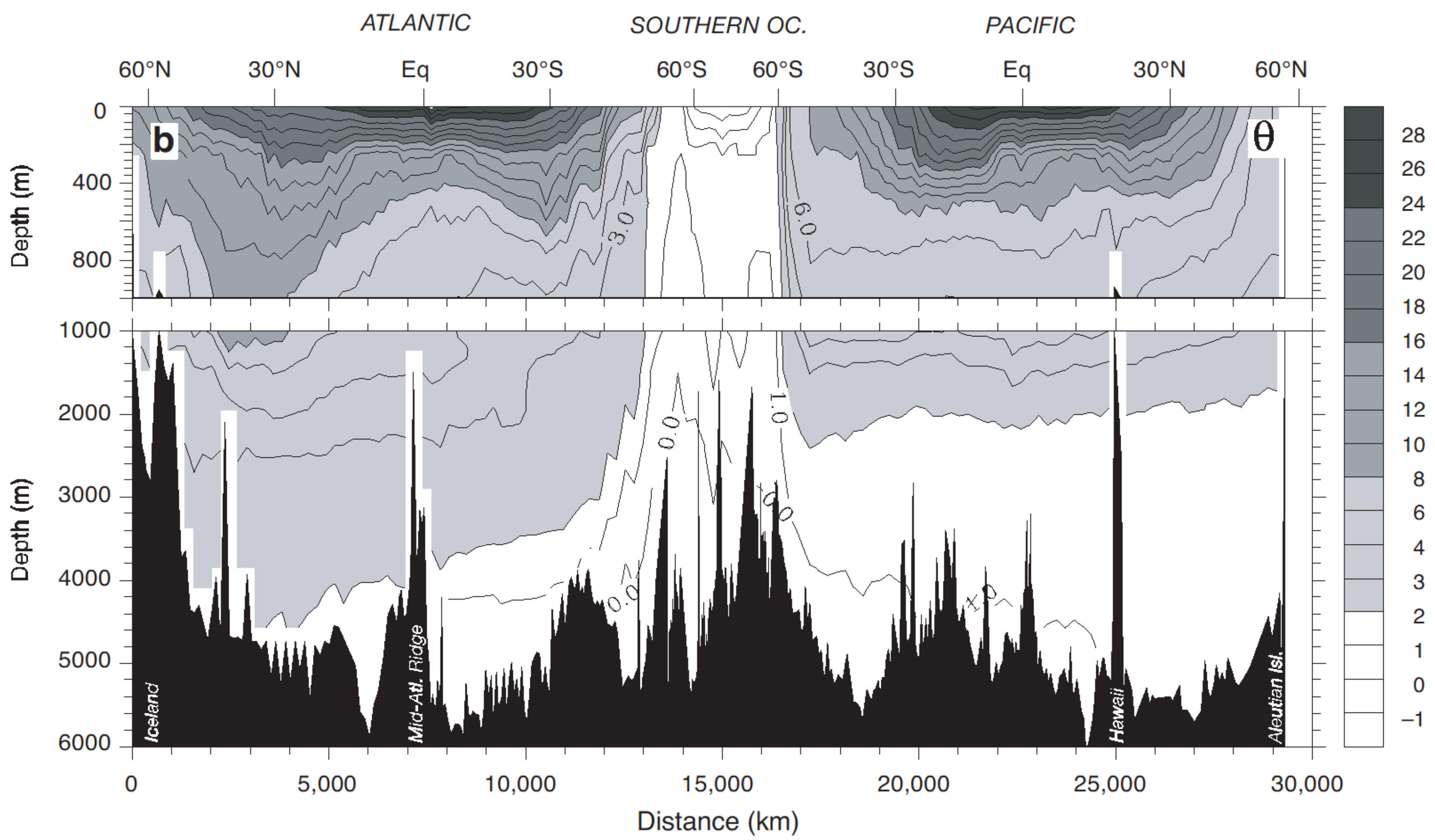

$\Delta^{14}C$

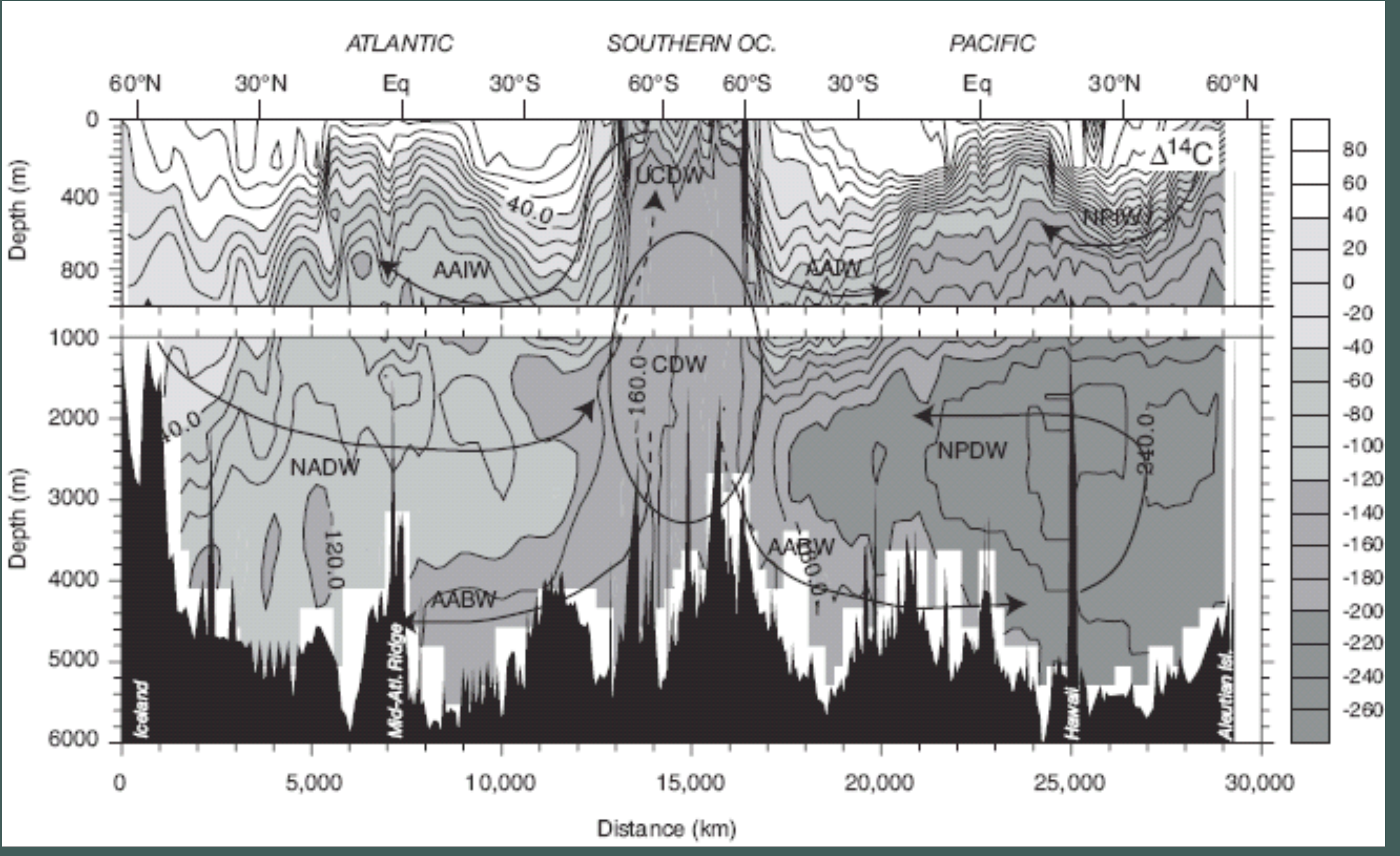

ATLANTIC
SOUTHERN OC.
PACIFIC
60°N
30°N
Eq
30°S
60°S
60°S
30°S
Eq
30°N
60°N
Δ14C
UCDW
40.0
AAIW
AAIW
NPIW
CDW
160.0
NADW
40.0
NPDW
240.0
120.0
AABW
AABW
Iceland
Mid-Atl. Ridge
Hawaii
Aleutian Isl.
Depth (m)
Depth (m)
0
400
800
1000
2000
3000
4000
5000
6000
0
5,000
10,000
15,000
20,000
25,000
30,000
Distance (km)
80
60
40
20
0
-20
-40
-60
-80
-100
-120
-140
-160
-180
-200
-220
-240
-260

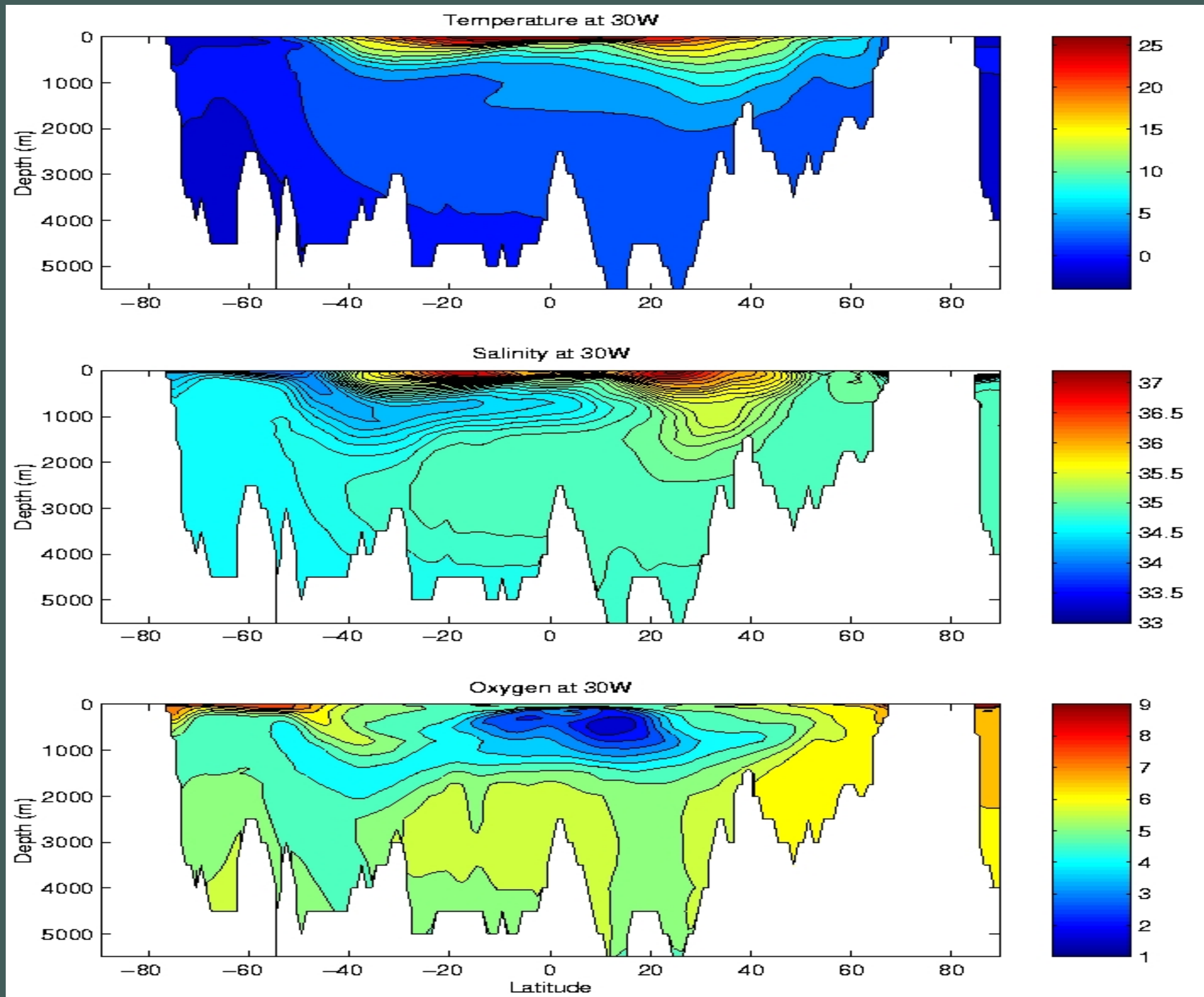

North-south sections of (a) temperature, (b) salinity, and (c) oxygen along the 30*o*W transect in the Atlantic ocean. Note the salinity tongues indicating the interleaving of water masses from sources in the Antarctic and the North Atlantic.

Atlantic

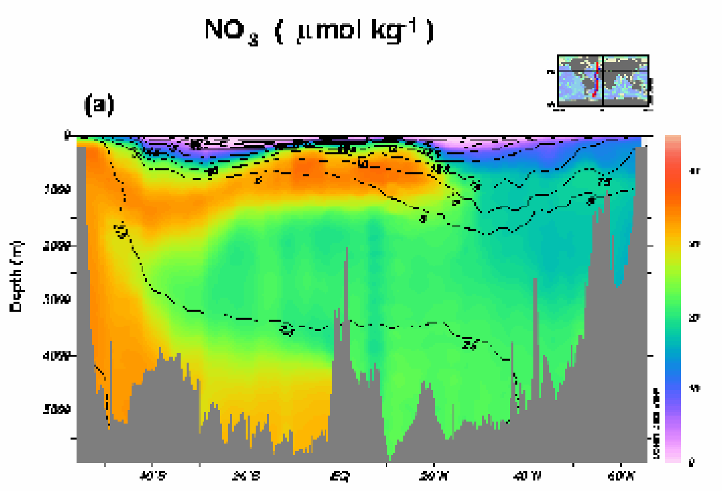

WOCE A16

Pacific

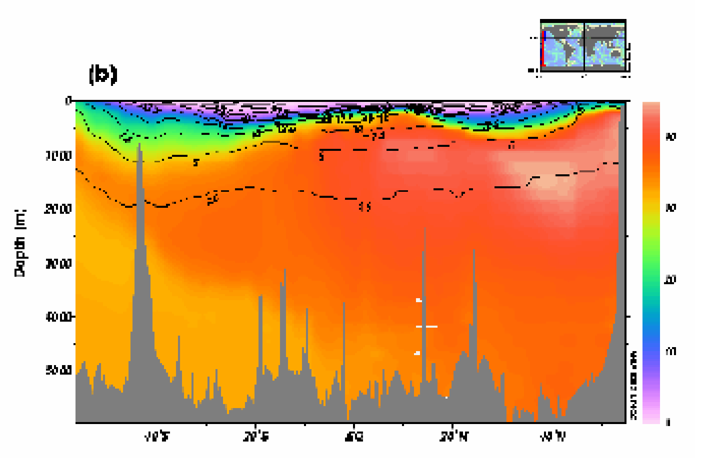

WOCE P15

- The overturning circulation determines the global distribution of temperature, salinity, oxygen…
- However, on seasonal to interannual time scales biological productivity is more sensitive to the basin-scale gyre circulation and to convective activities

Tracer conservation equation

$$\frac{\partial C}{\partial t} = \text{Advection} + \text{diffusion} + \text{reaction}$$

The advection due to the large scale circulation (wind-driven + MOC) explains the average distribution of chemicals in the absence of biological reactions

Reactions for a simple planktonic ecosystem

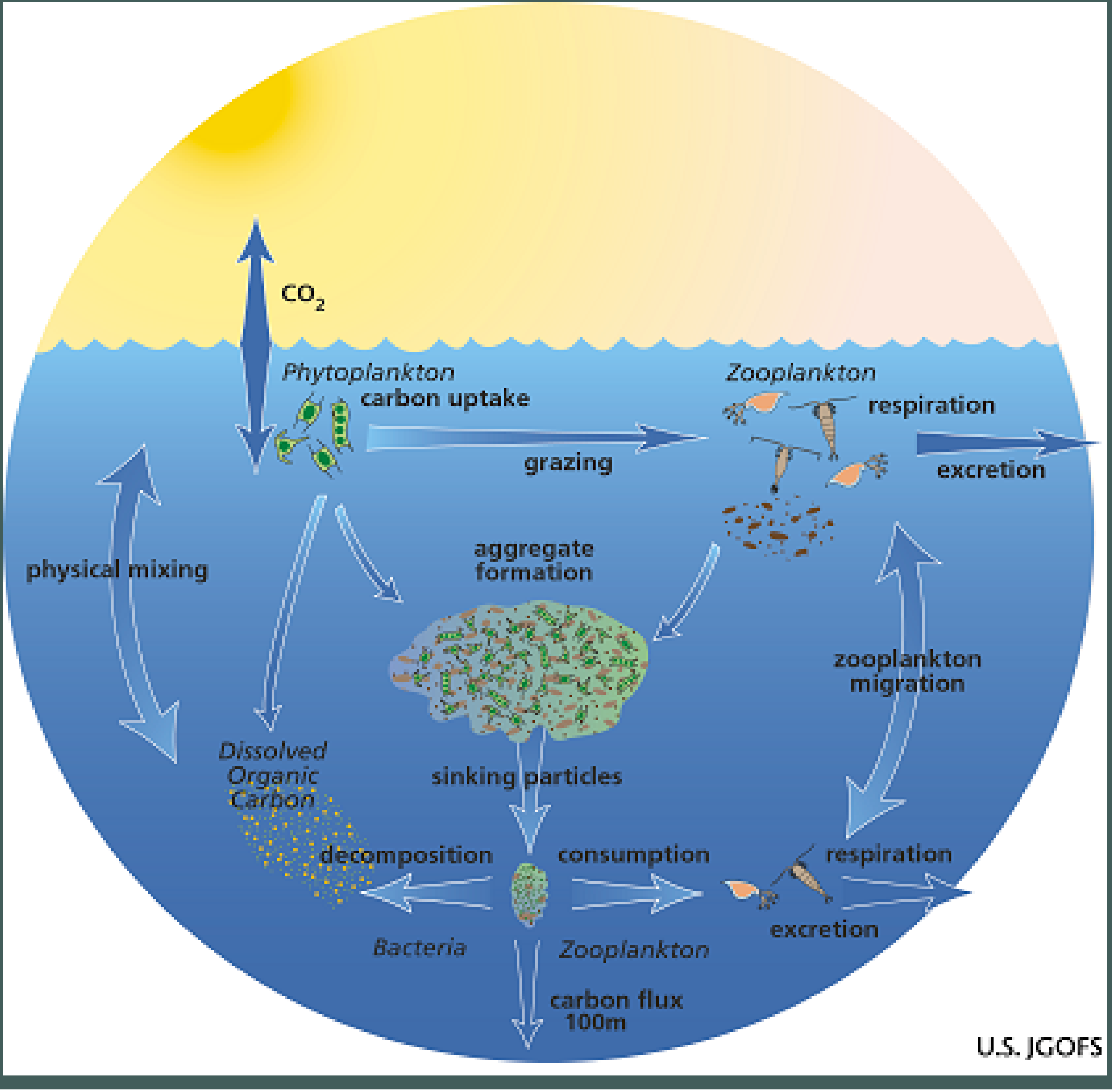

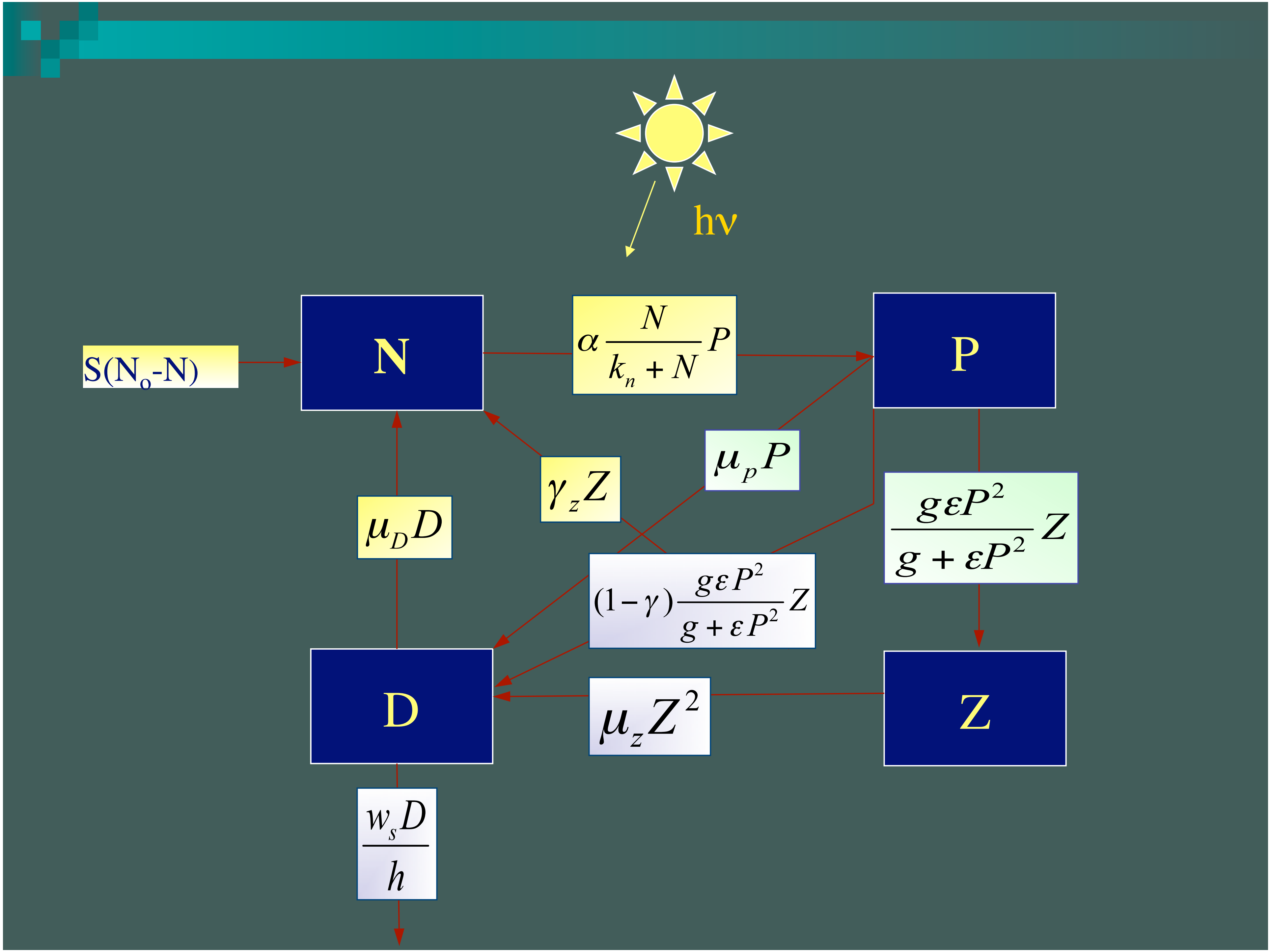

hν
S(No-N)
N
$\alpha \frac{N}{k_n + N} P$
P
$\mu_p P$
$\gamma_z Z$
$\mu_D D$
$\frac{g\varepsilon P^2}{g + \varepsilon P^2} Z$
$(1-\gamma)\frac{g\varepsilon P^2}{g + \varepsilon P^2} Z$
D
$\mu_z Z^2$
Z
$\frac{w_s D}{h}$

$$\frac{dN}{dt} = s(N_0 - N) - \alpha \frac{N}{k+N} P + \mu_D D + \gamma_Z Z$$

$$\frac{dP}{dt} = \alpha \frac{N}{k+N} P - \frac{g\varepsilon P^2}{g + \varepsilon P^2} Z - \mu_P P$$

$$\frac{dZ}{dt} = \gamma \frac{g\varepsilon P^2}{g + \varepsilon P^2} Z - \gamma_Z Z - \mu_Z Z^2$$

$$\frac{dD}{dt} = (1-\gamma) \frac{g\varepsilon P^2}{g + \varepsilon P^2} Z + \mu_P P + \mu_Z Z^2 - \mu_D D - w_s D / H$$

$$\frac{d}{dt} = \frac{\partial}{\partial t} + u \frac{\partial}{\partial x} + v \frac{\partial}{\partial y}$$

Equations for the ecosystem model based on Fasham et al., 1990

Various sizes of plankton may interact in different ways

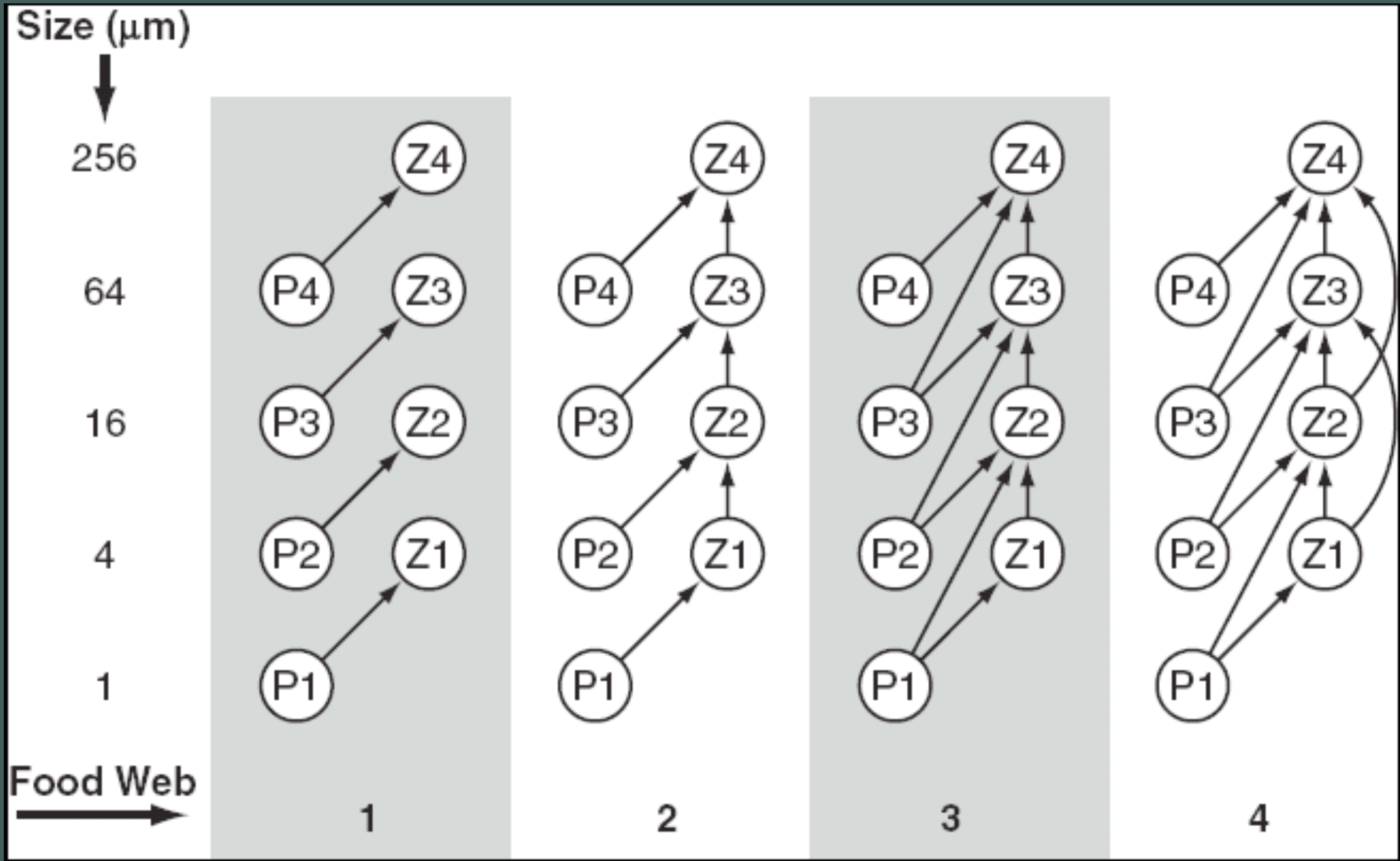

From Davis and Steele, 1994: an illustration of various ways that various size classes of P and Z may interact with each other

Problems:

- The expressions used to represent grazing, growing of P on N, mortality, sinking etc have been chosen more for their stability properties than for providing a realistic representation
- The stability properties are usually studied in stationary and homogeneous conditions
- The coefficients in the equations are very difficult to measure and depend on the species and location. Often are determined by fittings with sparse data or, even worse, lab (tank) experiments
- The use of multi-species models multiplies the number of unknowns.

Focusing on the averaged concentration of nitrate

observed

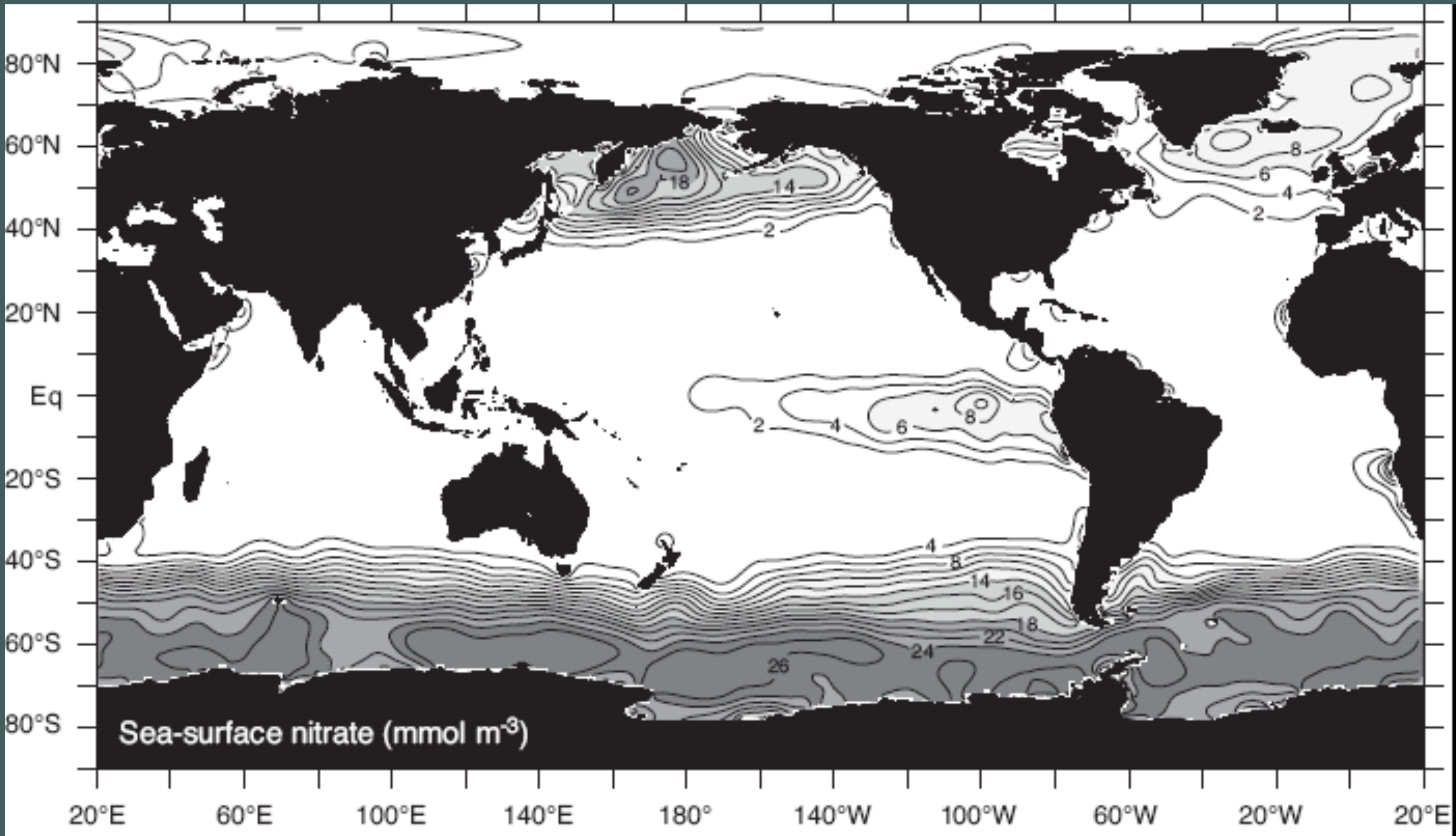

modeled distribution in the absence of biology

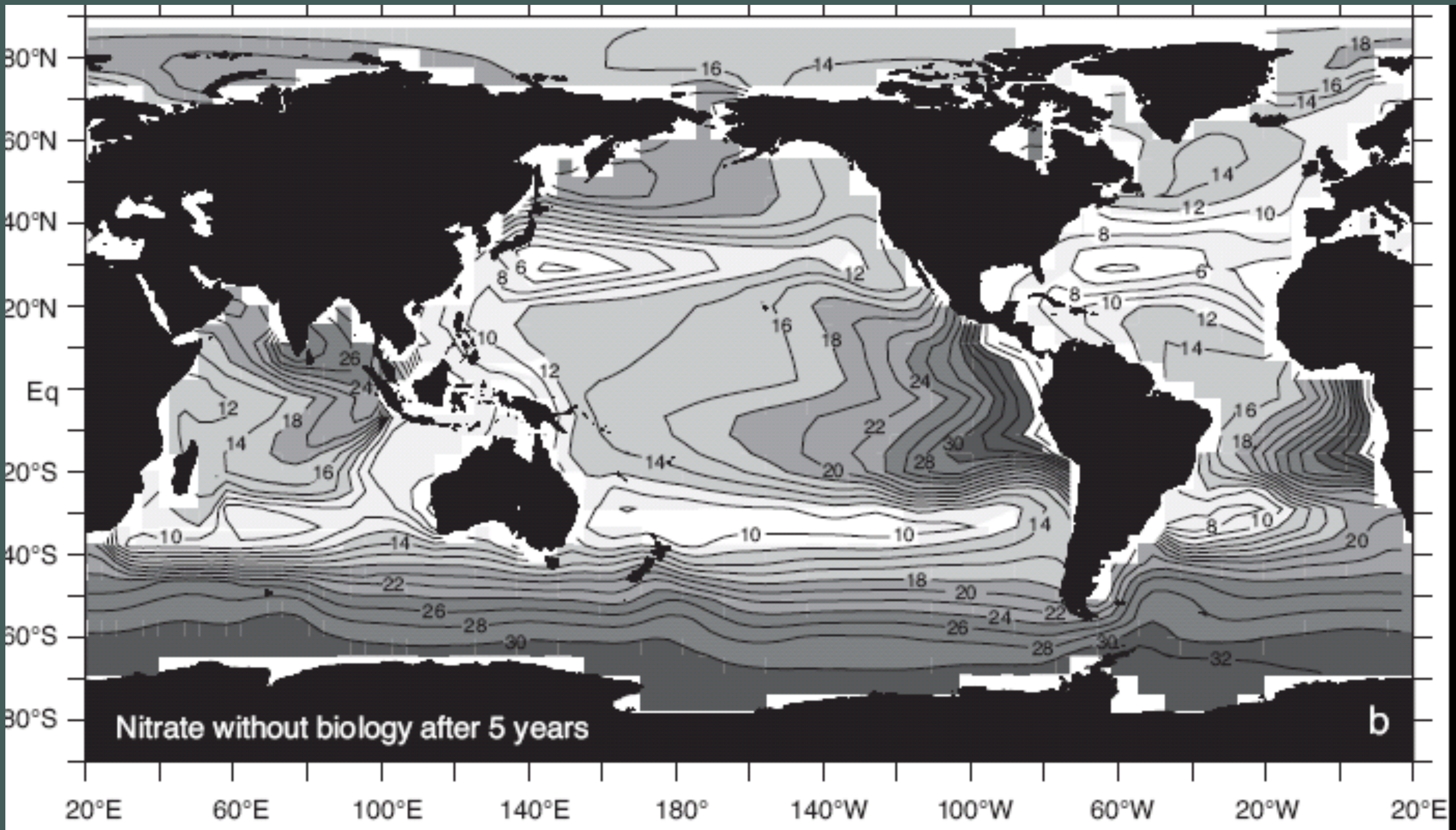

modeled distribution including biology

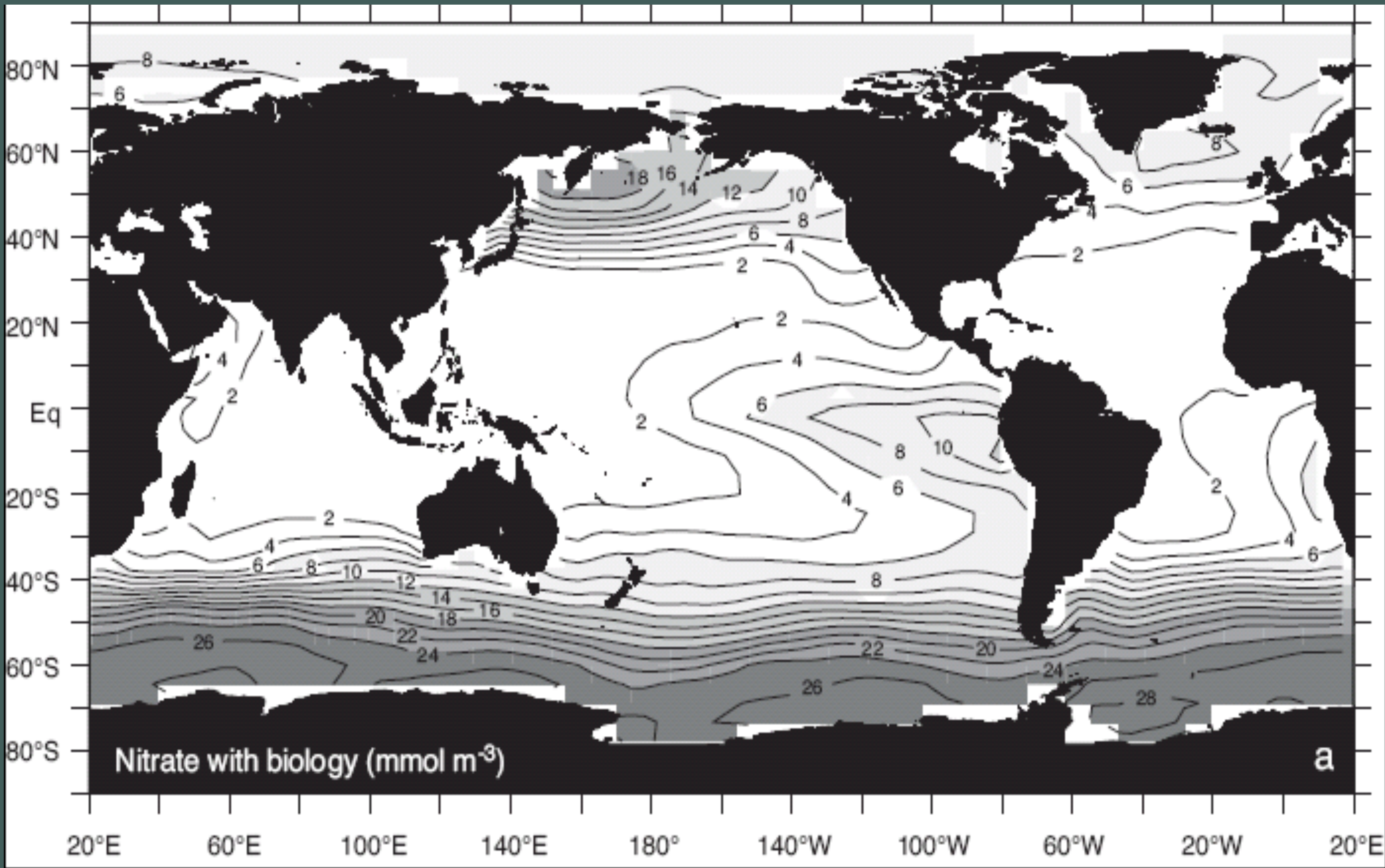

What else?

- Time-dependence: so far we considered the ocean circulation is in steady state. By including time dependence we add a rich set of additional behaviors: waves, eddies, convection, ocean-atmosphere interactions and various modes of variability from intraseasonal to inderdecadal (ENSO, NAO, SO, NPGO etc….)
- (Diffusion – molecular, turbulent diffusion...)
- Reaction

ENSO

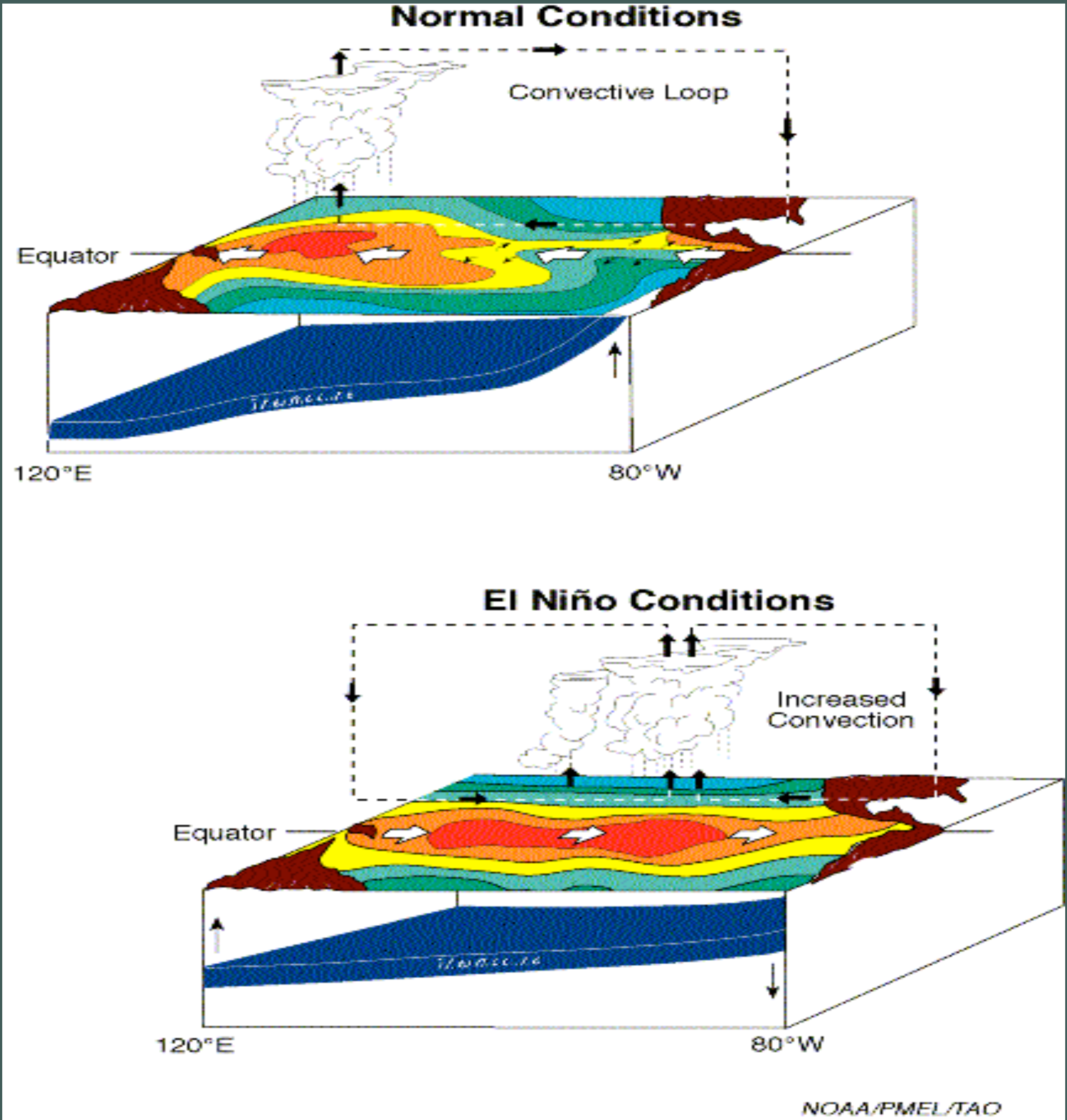
Normal Conditions
Convective Loop
Equator
120°E
80°W
El Niño Conditions
Increased Convection
Equator
120°E
80°W
NOAA/PMEL/TAO

La Nina conditions

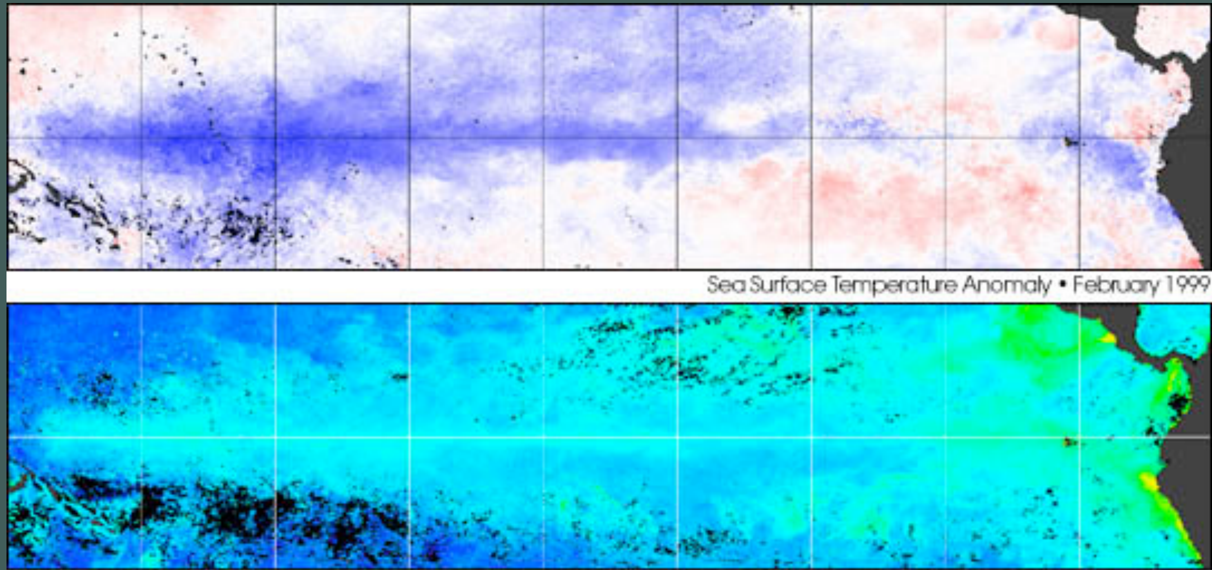

Sea Surface Temperature Anomaly • February 1999

Chlorophyll a Concentration • February 1999

El Nino conditions

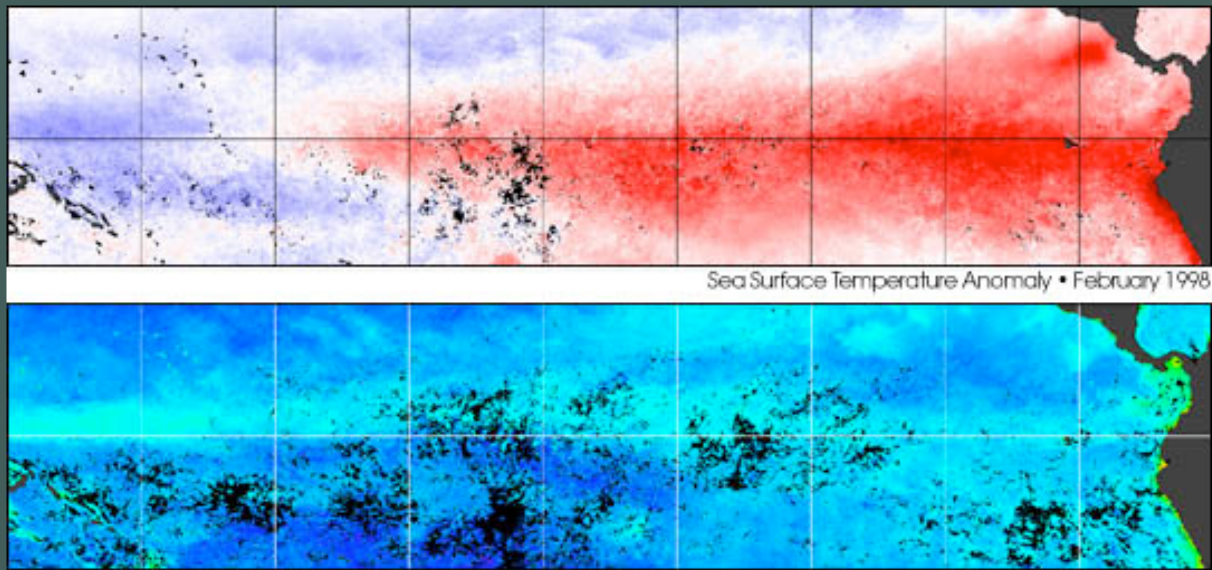

Sea Surface Temperature Anomaly • February 1998

Chlorophyll a Concentration • February 1998

The NPGO
(North Pacific Gyre Oscillations)

Di Lorenzo et al. GRL 2008

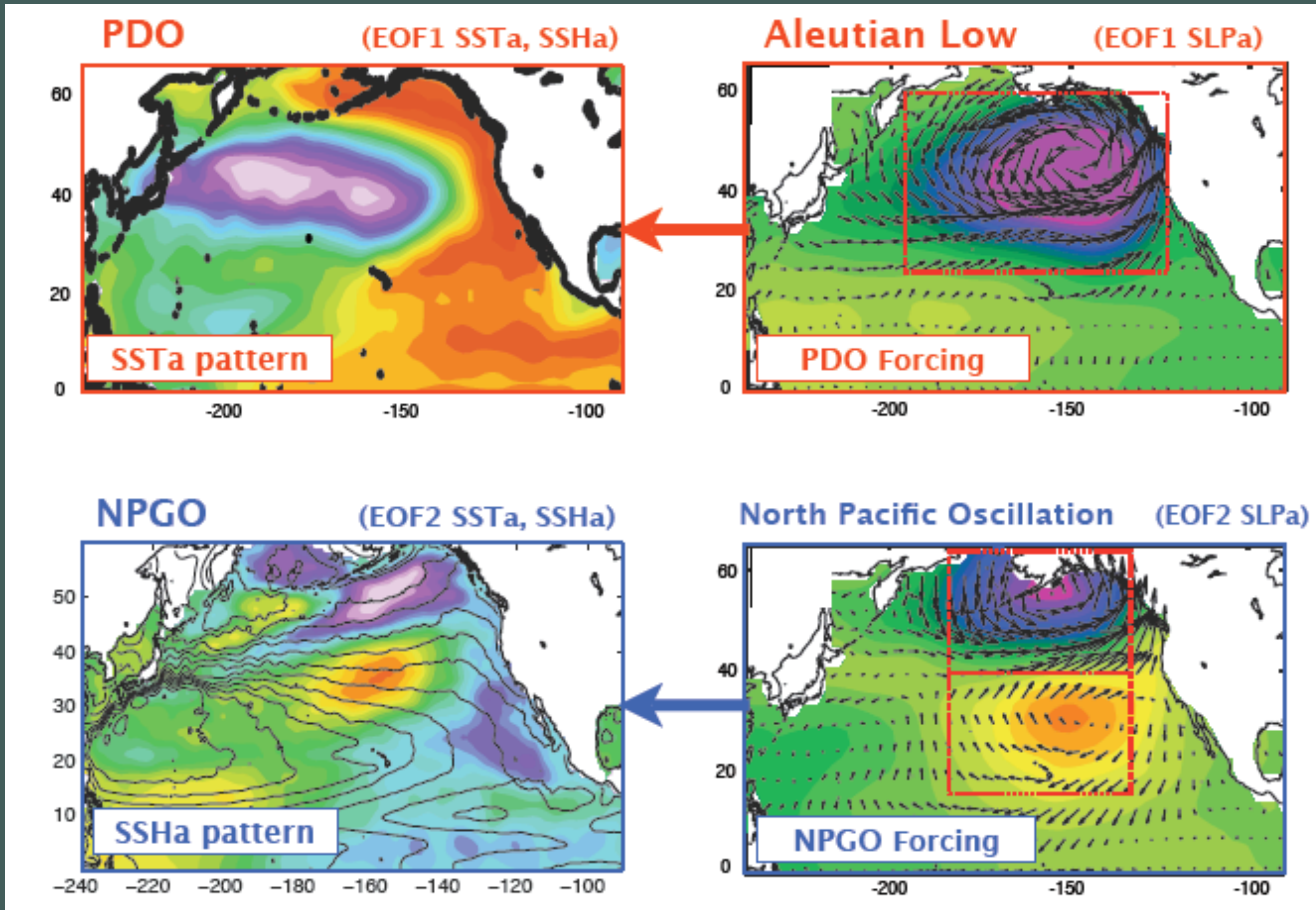

North Pacific dominant mode of oceanic variability: the PDO and NPGO (left), are driven by the first two dominant modes of atmospheric variability evident in sea level pressure, the Aleutian Low variability and the NPO (right).

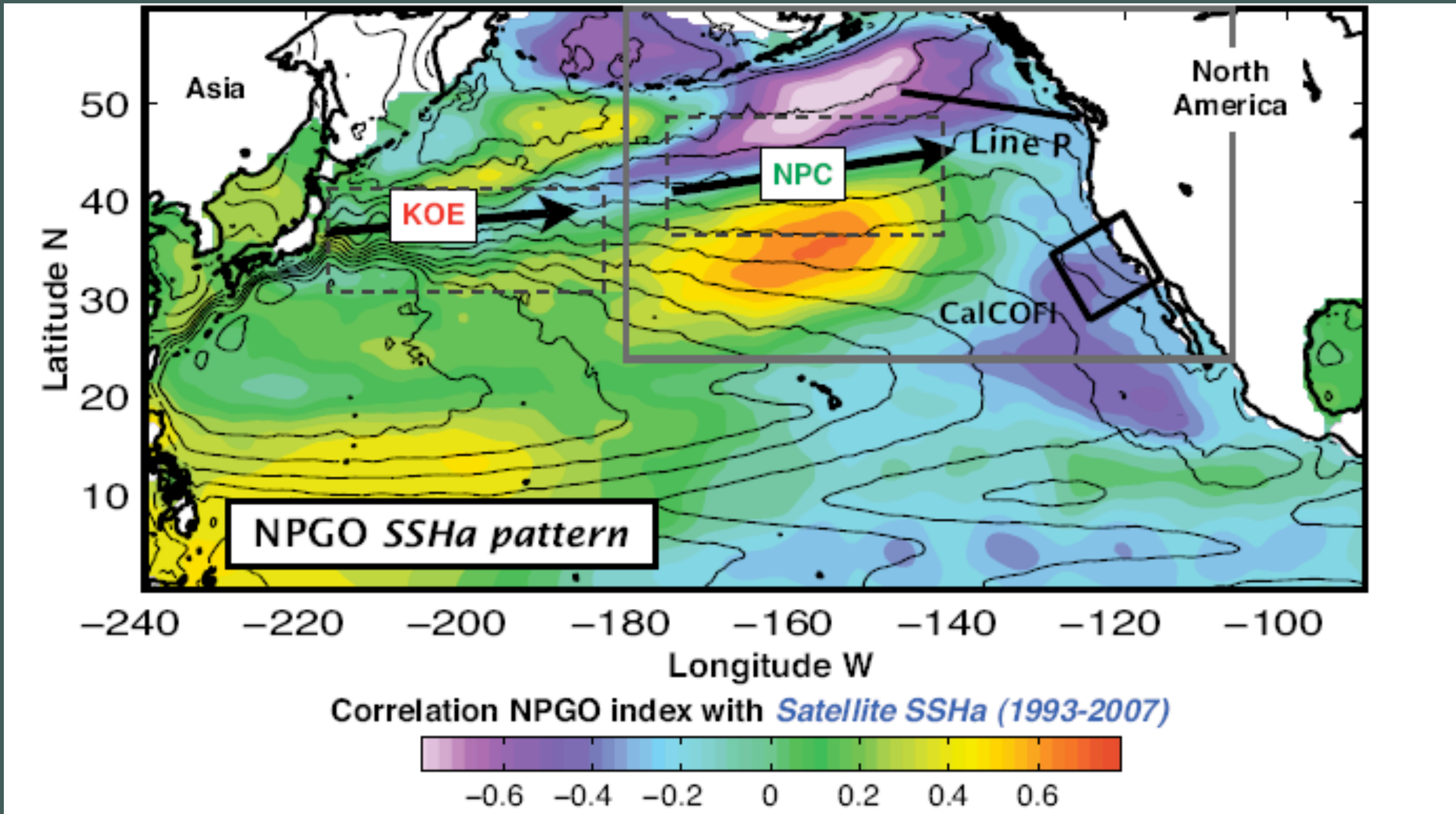

Asia
North America
Line P
NPC
KOE
CalCOFI
NPGO SSHa pattern
Latitude N
50
40
30
20
10
−240 −220 −200 −180 −160 −140 −120 −100
Longitude W
Correlation NPGO index with Satellite SSHa (1993-2007)
−0.6 −0.4 −0.2 0 0.2 0.4 0.6

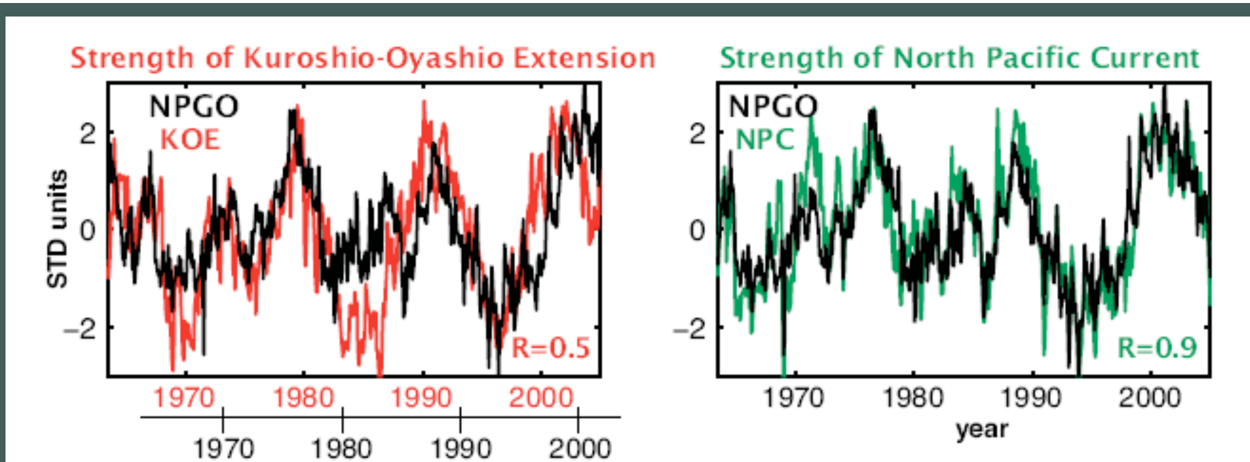

Strength of Kuroshio-Oyashio Extension
NPGO
KOE
STD units
2
0
−2
R=0.5
1970 1980 1990 2000
1970 1980 1990 2000
Strength of North Pacific Current
NPGO
NPC
2
0
−2
R=0.9
1970 1980 1990 2000
year

Di Lorenzo
et al.
GRL 2009

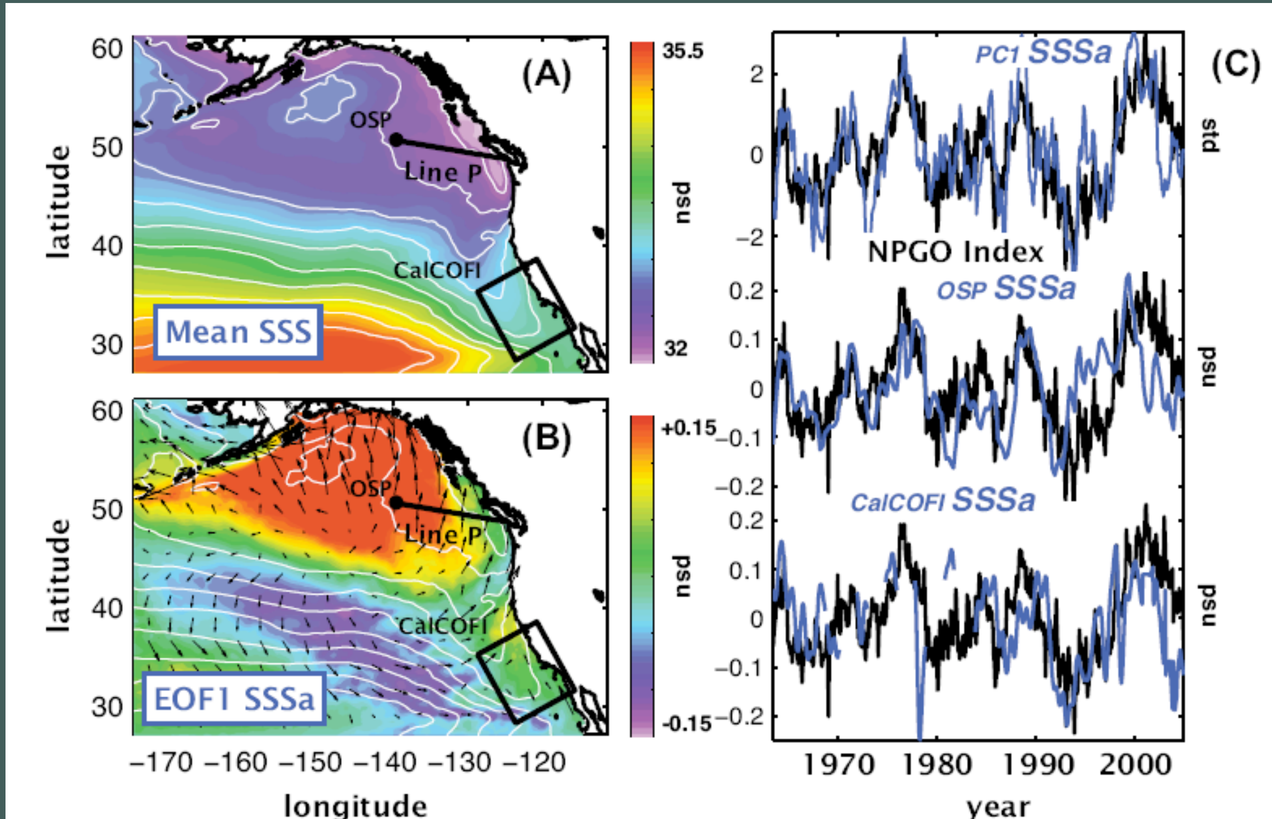

(A) Mean surface salinity (SSS) from ROMS model over the period 1950-2004. (**B**) First mode of variability for model surface salinity anomaly (SSSa) inferred from EOF1. Black arrows correspond to surface currents anomalies during the positive phase of the NPGO. (**C**) Timeseries of NPGO index (black) compared to PC1 of SSSa (R=0.67, 99%), observed SSSa at ocean Station Papa (OSP) (R=0.40, 96%) at the offshore end of Line-P [*Crawford et al., 2007*], and observed SSSa from CalCOFI program (R=0.42, 95%).

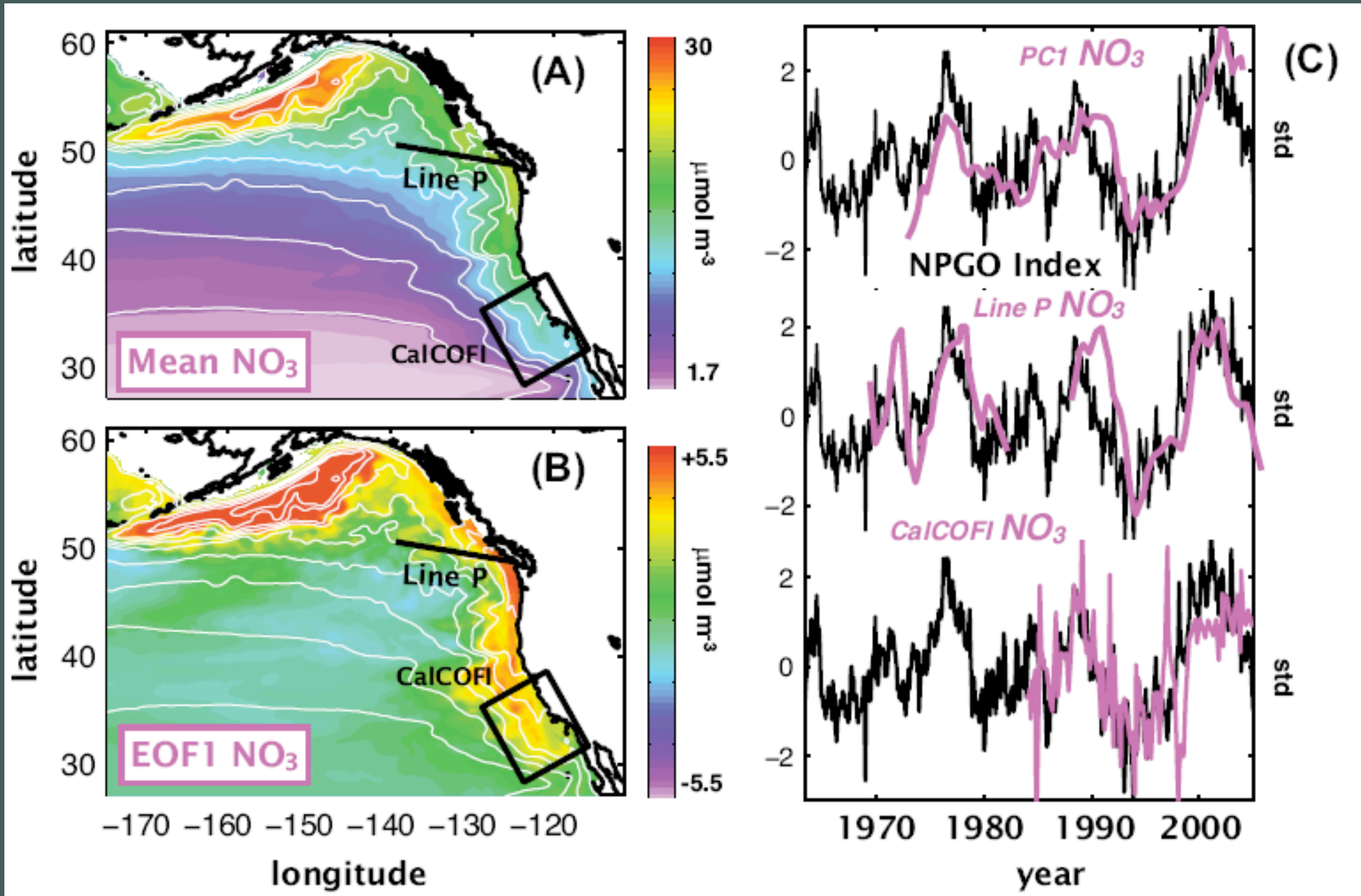

Variability of subsurface nitrate (NO3). (A) Mean subsurface (150m) NO3 from ROMS model over 1975-2004. (**B**) First mode of variability for model subsurface (150m) NO3 anomaly inferred from EOF1. (**C**) Timeseries of NPGO index (black) compared to PC1 of NO3 (R=0.65, 99%), observed mix layer NO3 at Line-P [*Peña and Varela, 2007*], and observed NO3 from CalCOFI program (R=0.51, 95%).

Mesoscale variability (10-200km)

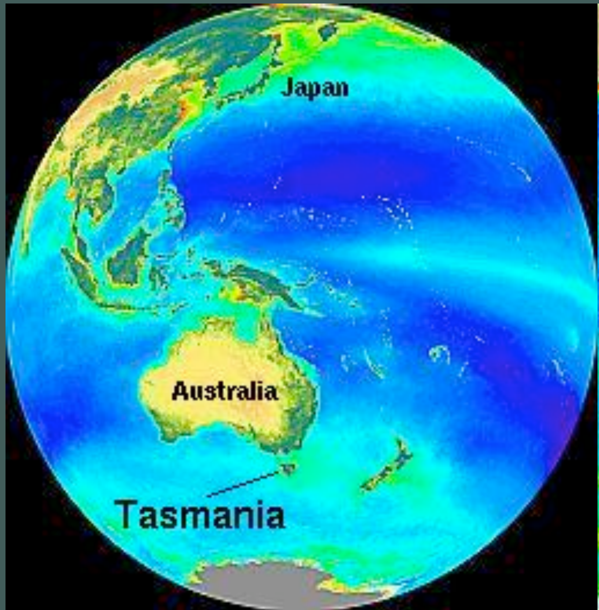

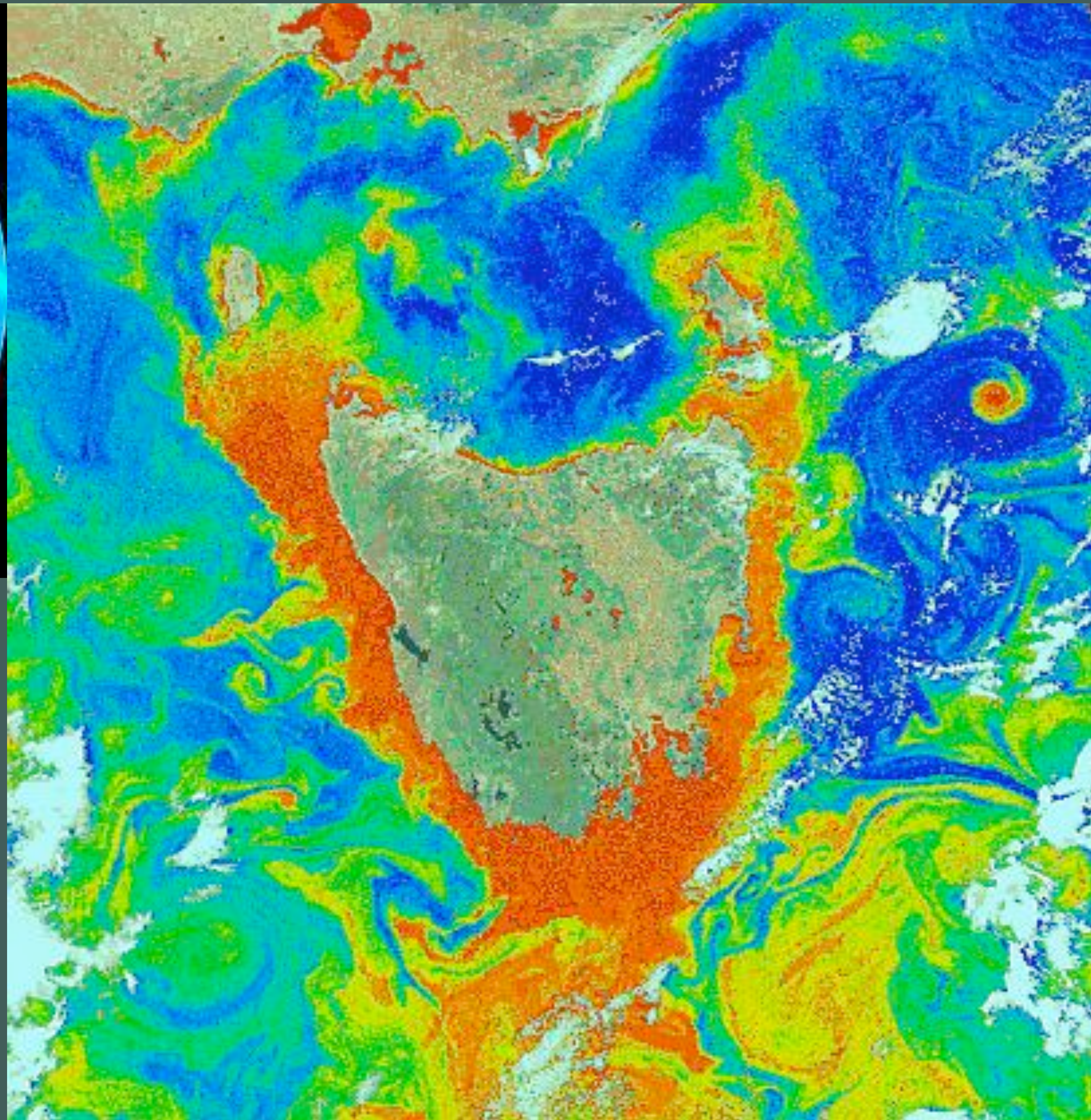

image of chlorophyll concentration around Tasmania in 1981 (Coastal Zone Color Scanner – CZCS)

Plankton bloom in a Gulf Stream shear zone within eddies in a 250-mm-lens view of the Atlantic Ocean in May 1985.

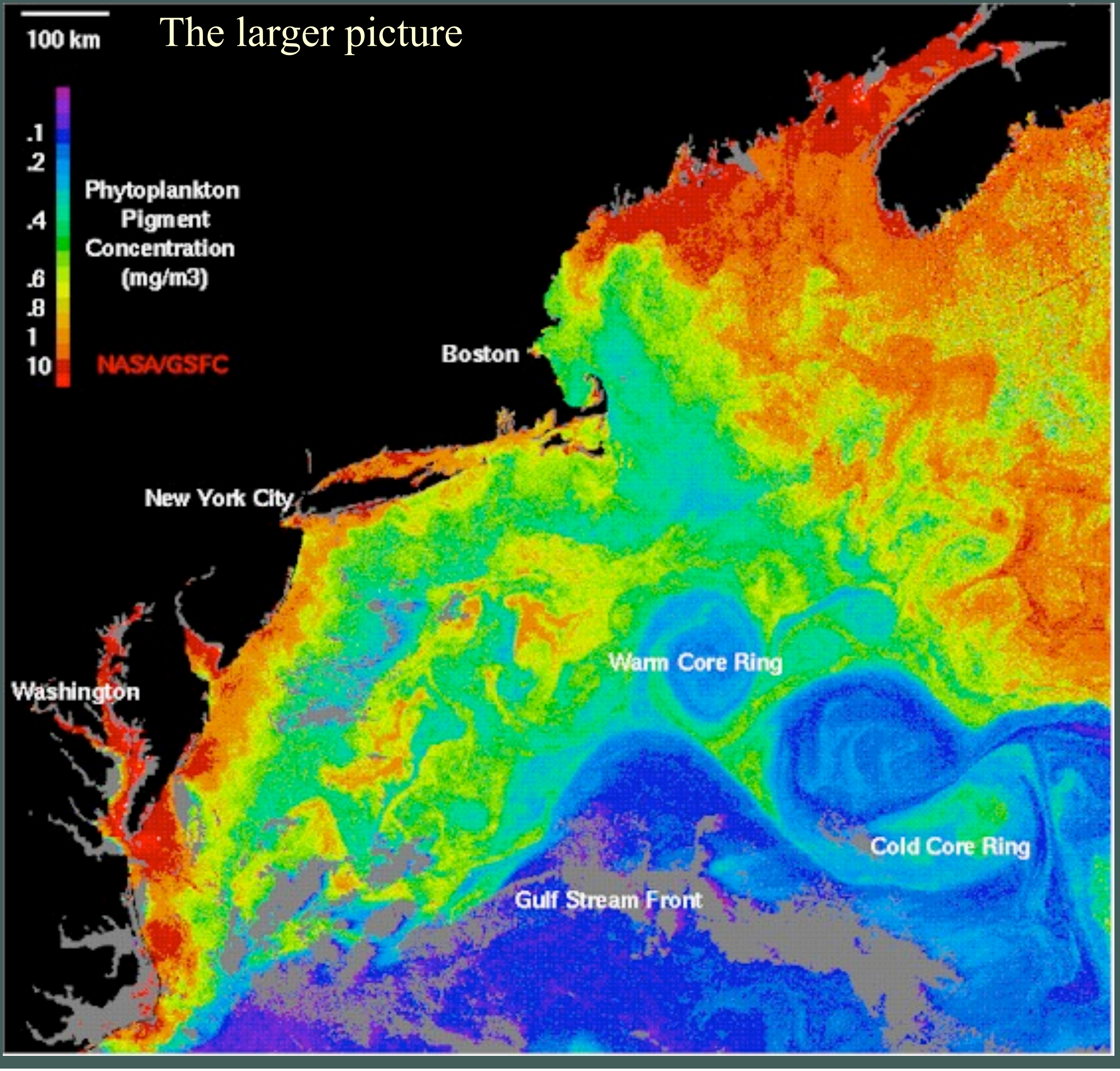

100 km
The larger picture
.1
.2
.4
.6
.8
1
10
Phytoplankton Pigment Concentration (mg/m3)
NASA/GSFC
Boston
New York City
Washington
Warm Core Ring
Cold Core Ring
Gulf Stream Front

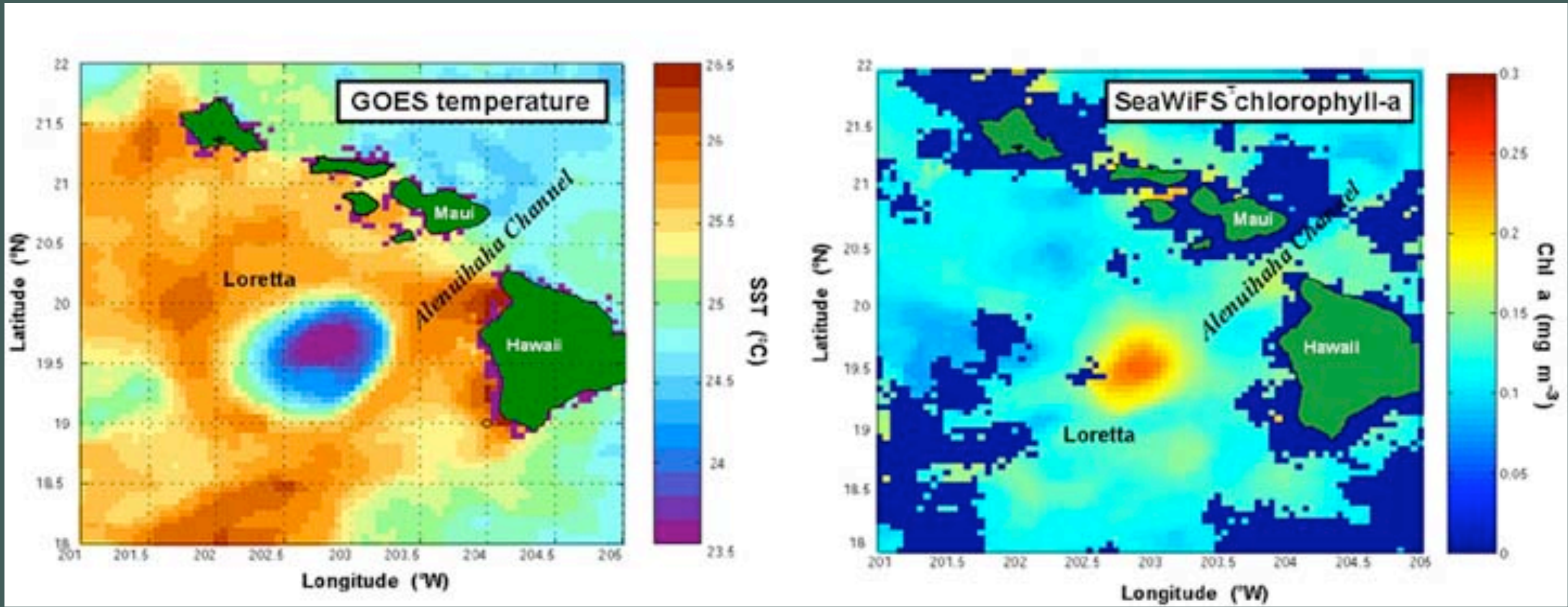

The ‘Loretta’ eddy in the Alenuihaha Channel between the islands of Hawaii and Maui .

LEFT: Two-day composite of GOES sea-surface temperature during 3-4 September 1999.

RIGHT: eight-day composite of SeaWiFS chlorophyll during 29 August - 5 September 1999.

Using a OGCM (MICOM)

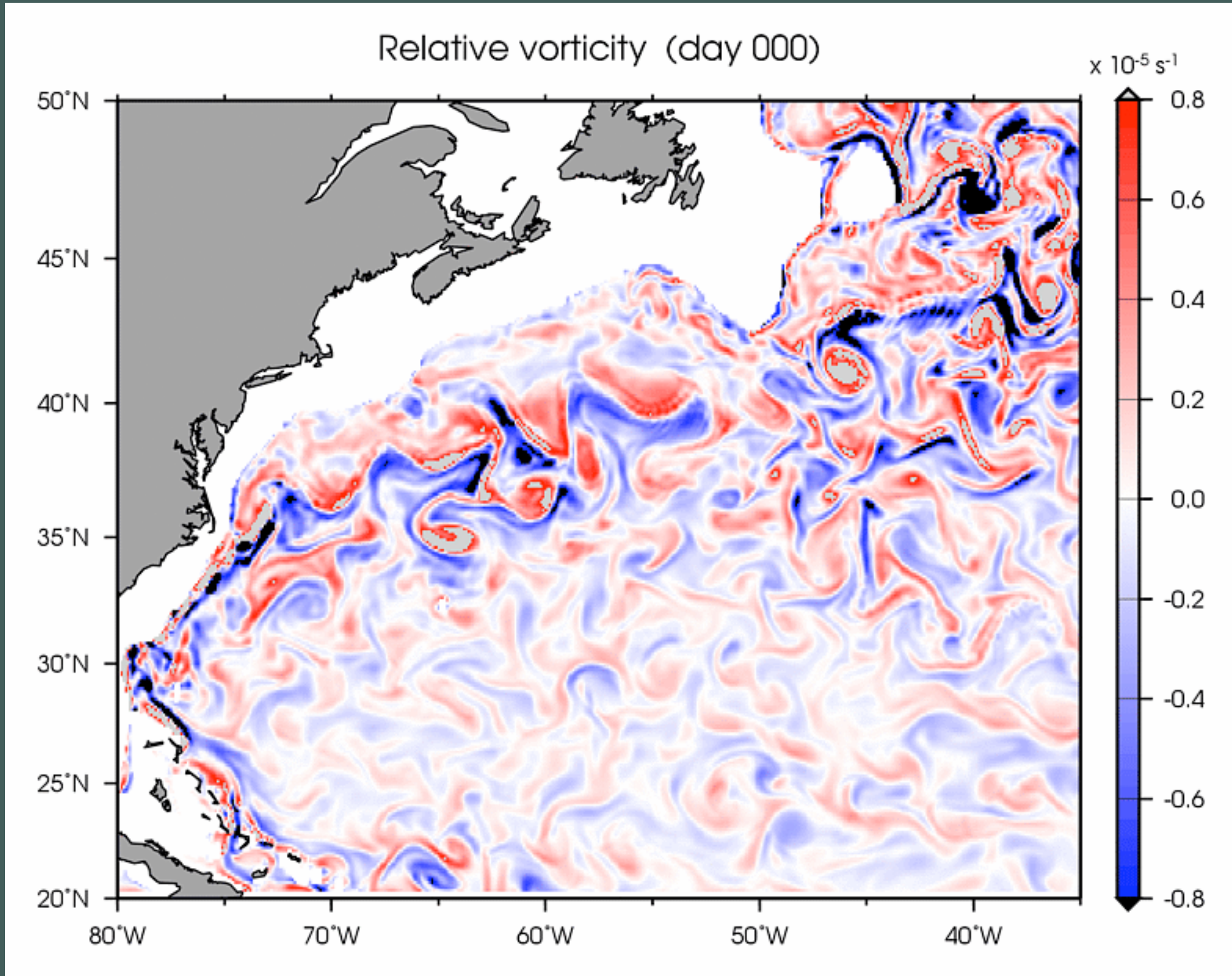

from Veneziani, Griffa, Garraffo, Chassignet, JMR, 2005

Fig. 2.1.
Schematic figure displaying one- and three-dimensional views of the physical processes affecting biological production: a In the vertical, there is a phytoplankton growth within the ecosystem, export of organic matter and remineralisation at depth, which is partly maintained through the physical transfer of nutrients within the ocean involving vertical advection, diapycnic diffusion and convection; b a more complete view includes the physical transfer of nutrients by the three-dimensional circulation involving contributions from the overturning, gyre, eddy and frontal circulations, as well as involving interactions with spatial variations in convection

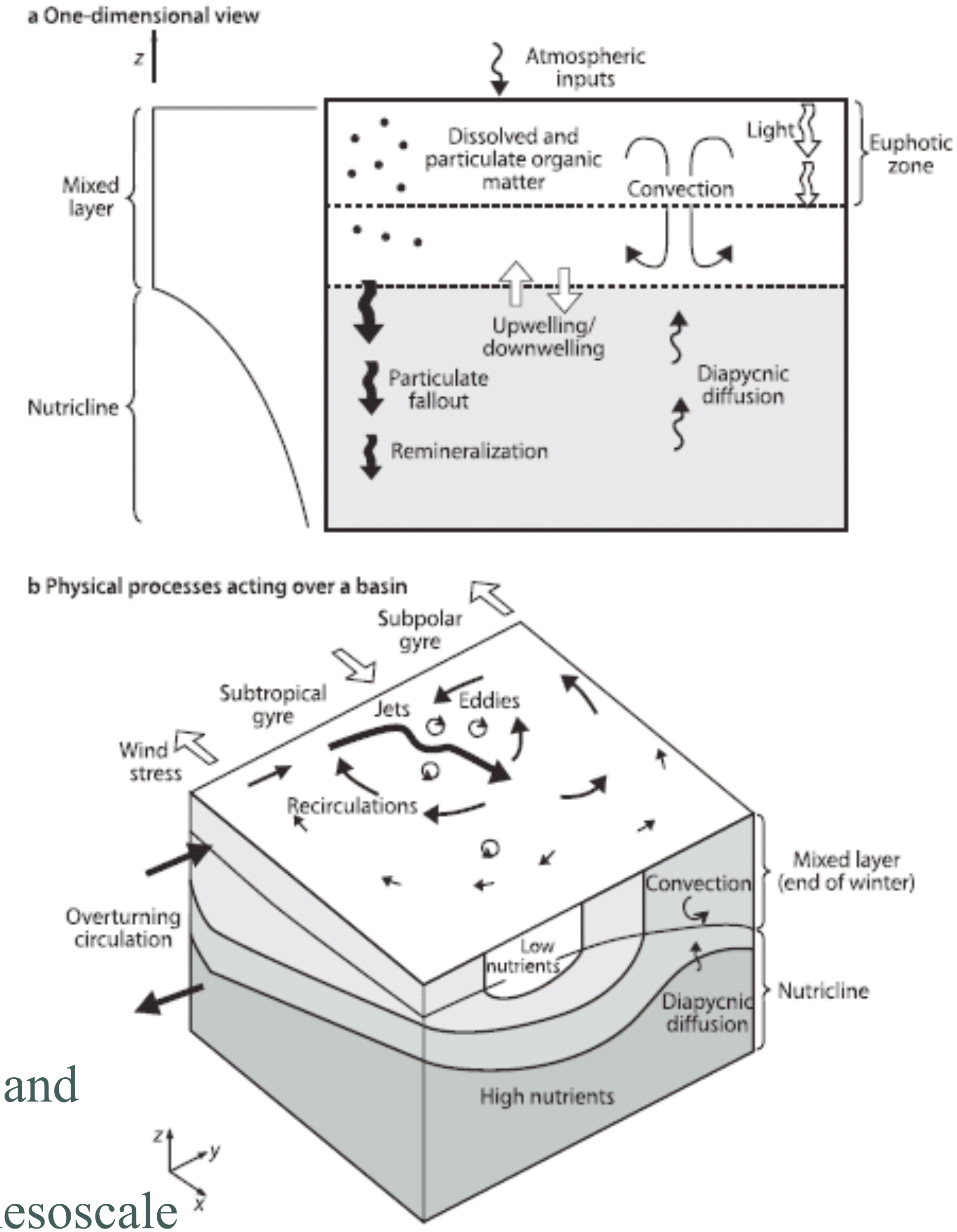

From Williams and Follows, 2003: Schematic of mesoscale processes involved in the plankton dynamics

Focusing on the eddies: Physical mechanism
Traditional view: geostrophic (balanced) flow

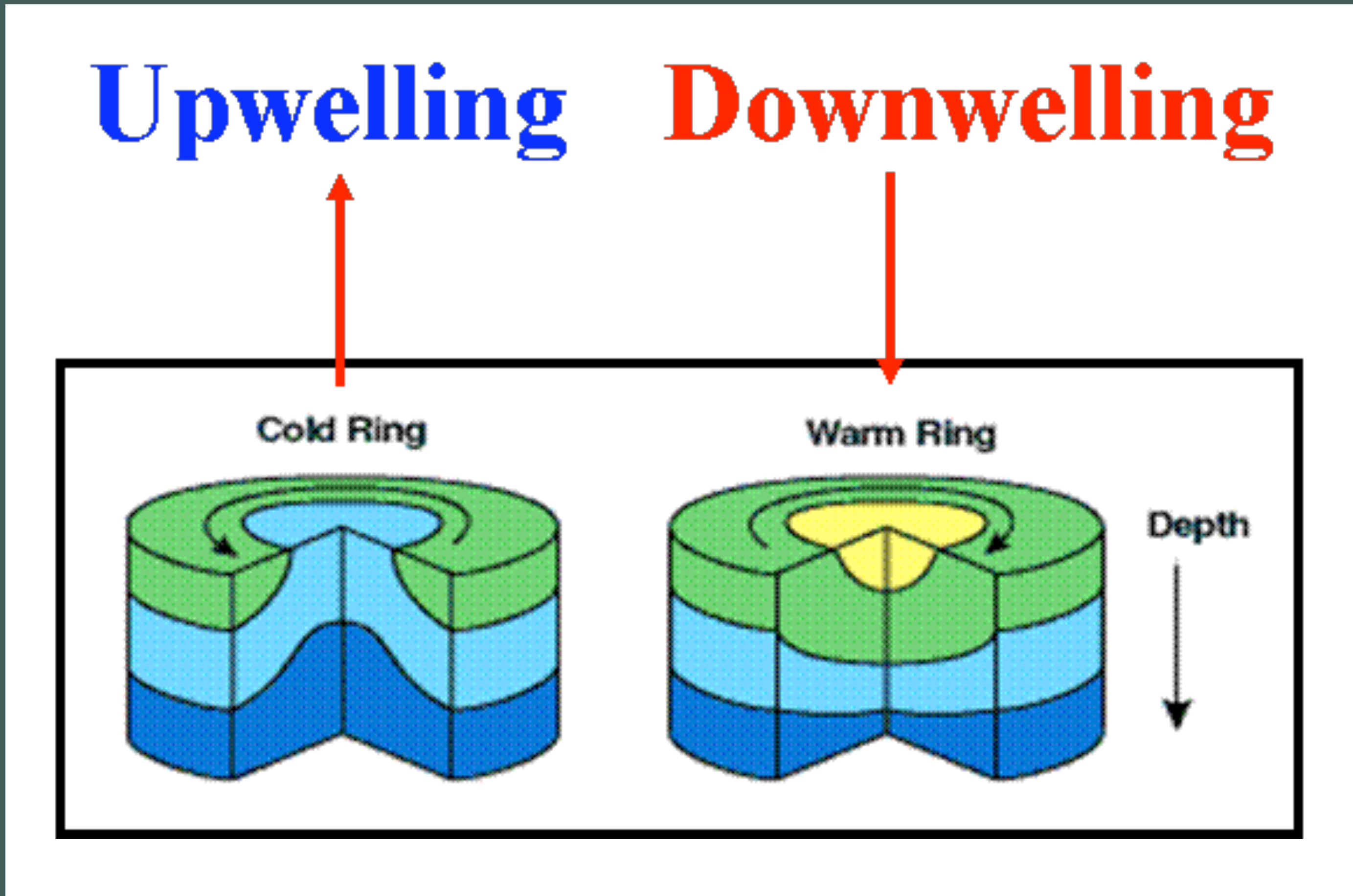

Both vertical and horizontal velocities are important.

A lot of work in the past decade (e.g. Falkowski et al., 1991; McGillicuddy et al., 1998; Oschlies and Garcon, 1998; Abraham, 1998; Abraham et al., 2000; Martin et al., 2002; Williams and Fasham, 2003)

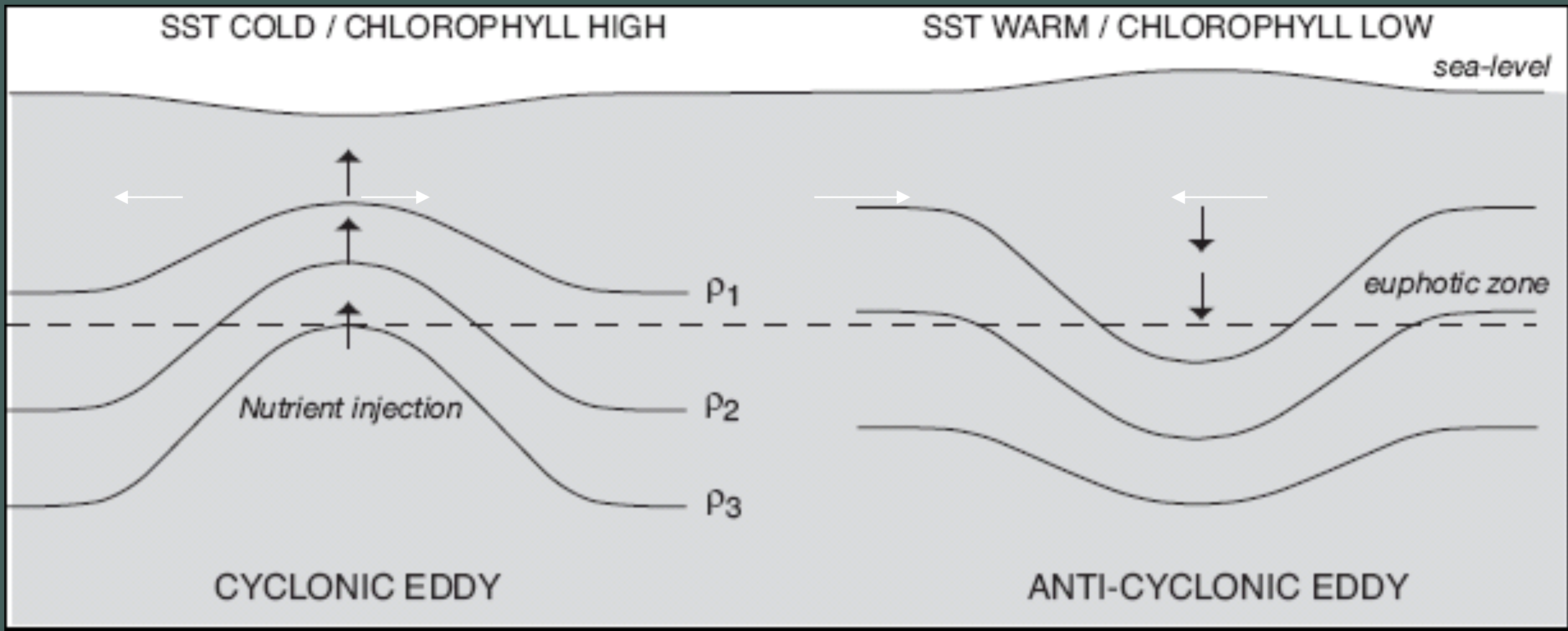

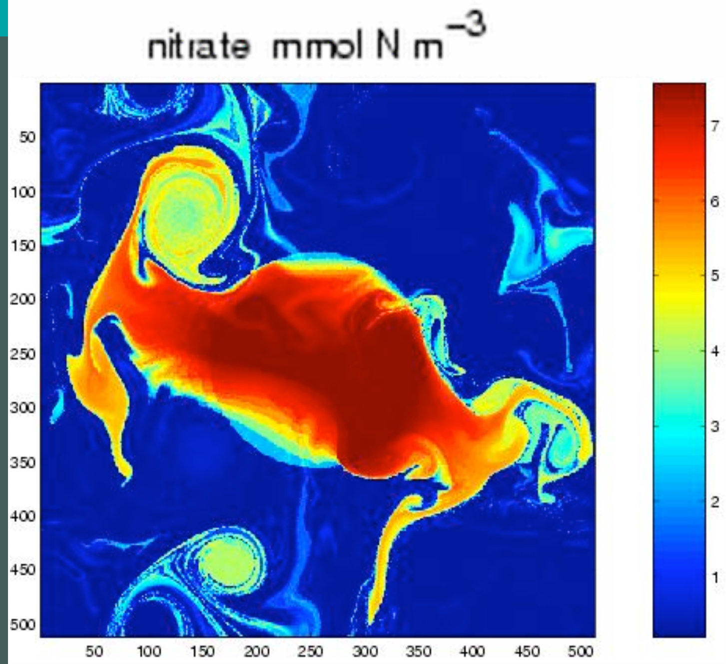

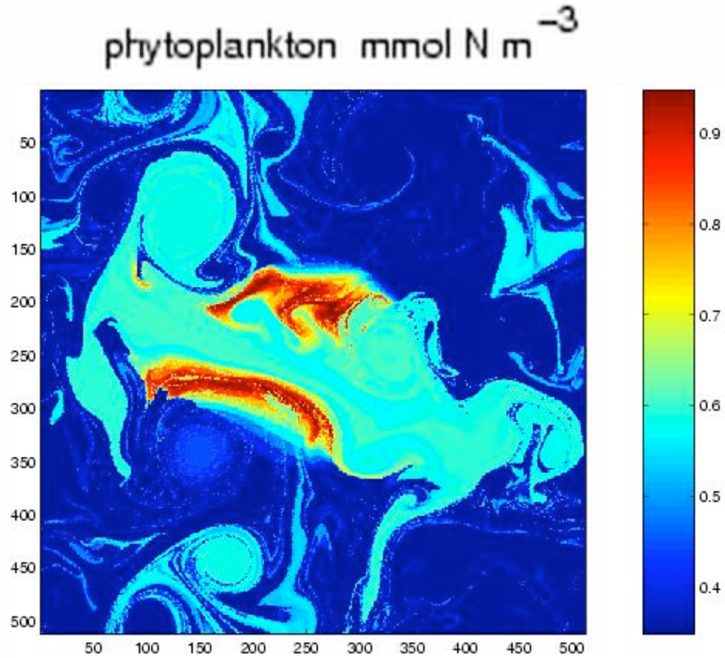

Increase in PP 29%

after 80 days

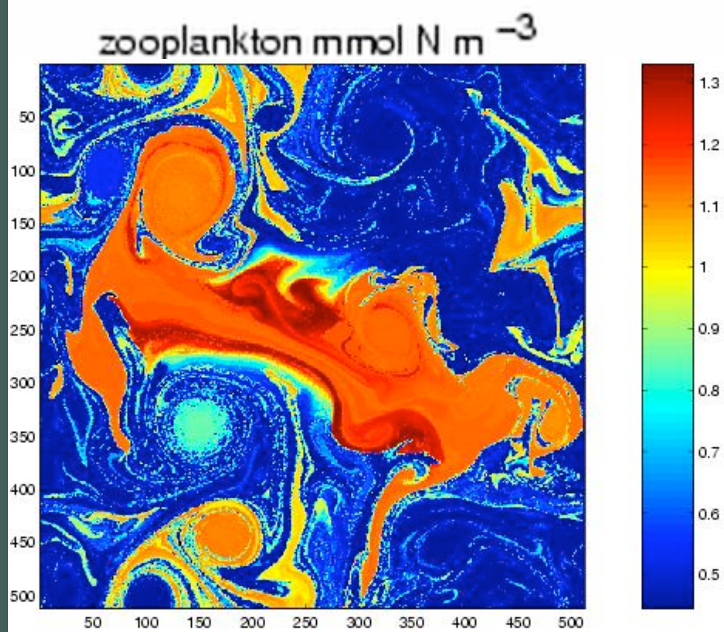

Martin, Richards, Bracco, Provenzale, GBC 2002

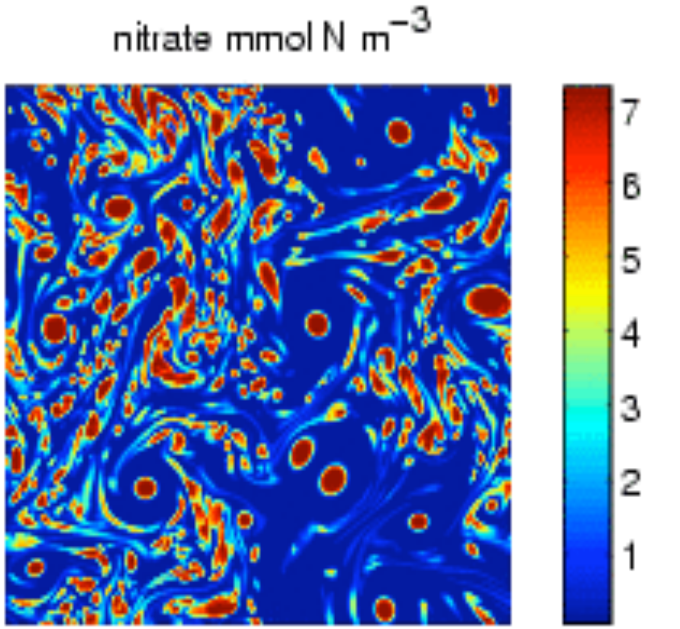

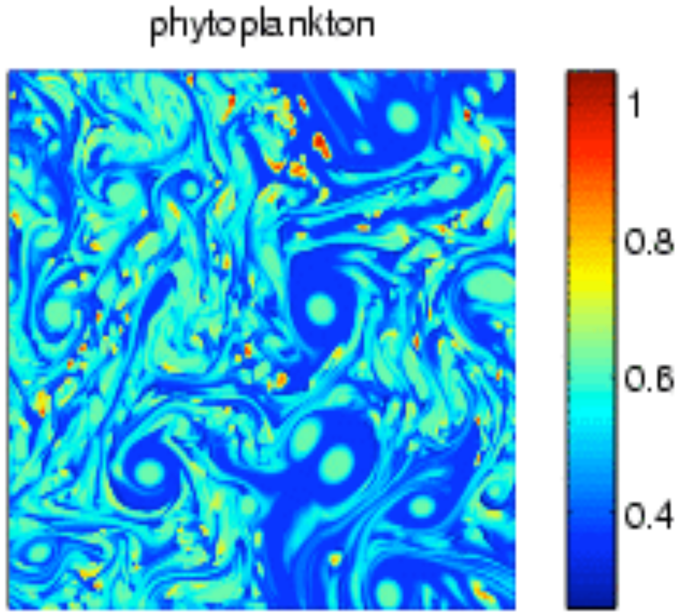

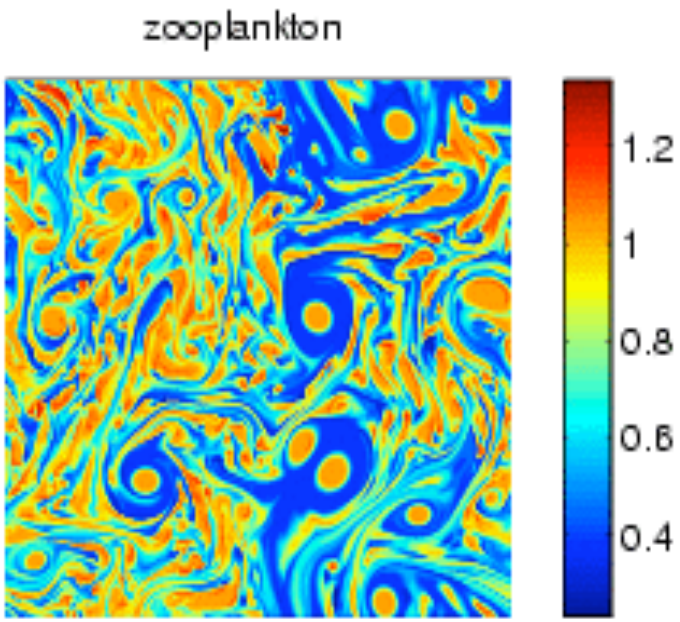

after 80 days, same total area for upwelling

Increase in PP 139%!

Eddies and fronts

Modelled new production (10^{-3} mol N m^{-2}) within the euphotic layer for a zonal jet undergoing baroclinic instability (Lévy et al. 2001). Snapshots of the new production are shown at days 14 and 22 for integrations at mesoscale (*upper panel*) and sub-mesoscale (*lower panel*) resolutions of 6 km and 2 km respectively. Over the integration, meanders develop leading to anticyclones to the north and cyclones to the south of the jet. The new production increases in intensity as the resolution increases and becomes concentrated along anticyclonic filaments. The area-averaged new production increases from 6.5 to 10.7×10^{-3} mol N m^{-2} as the resolution is increased from 6 km to 2 km; in comparison, the area-averaged new production only reaches 3.7×10^{-3} mol N m^{-2} if the resolution is reduced to 10 km

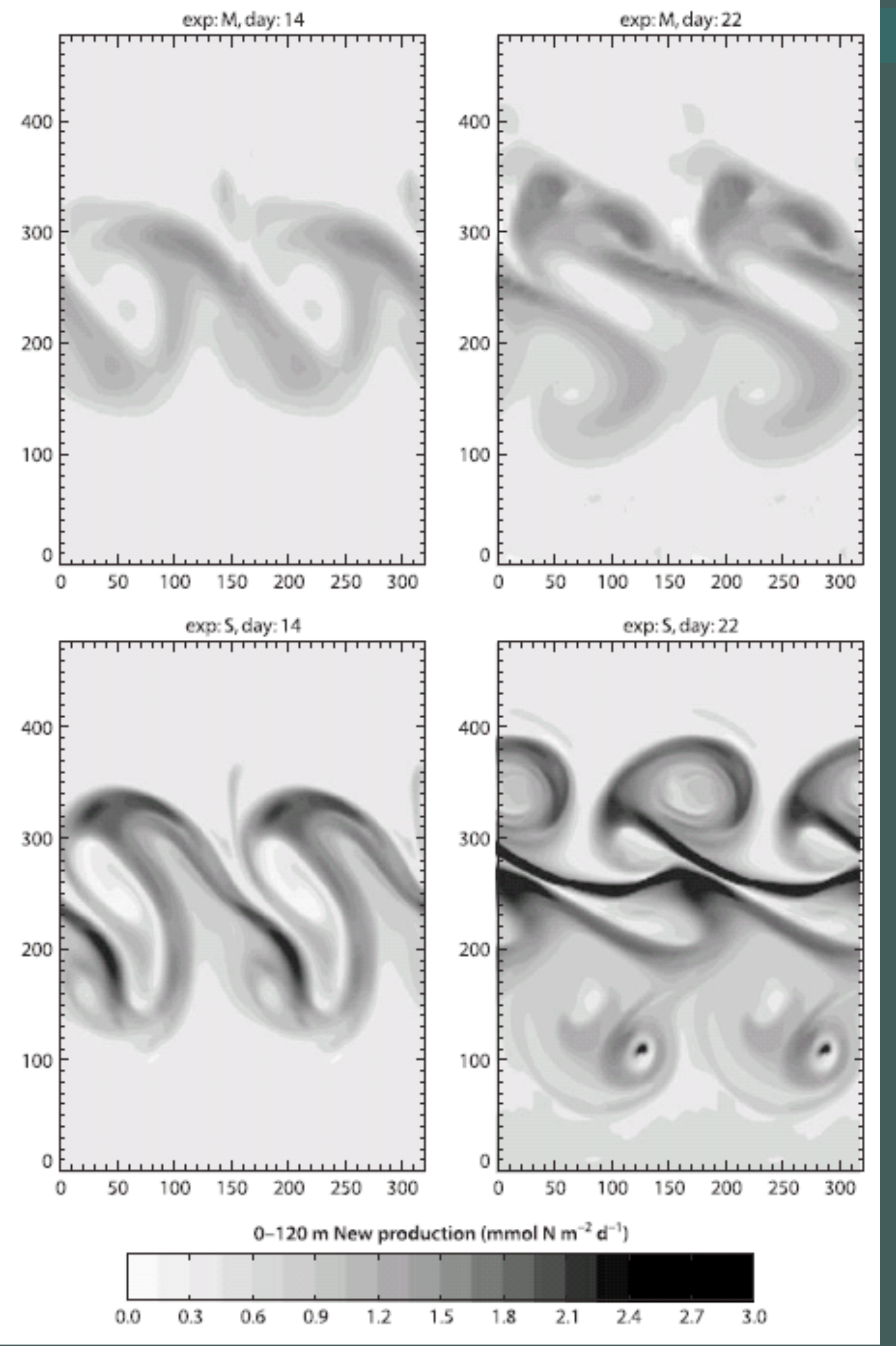

Moving to the submesoscale (1-10km): Ageostrophic (unbalanced) motions cannot be neglected

Klein and Lapyere, Ann. Rev. Marine Science, 2009

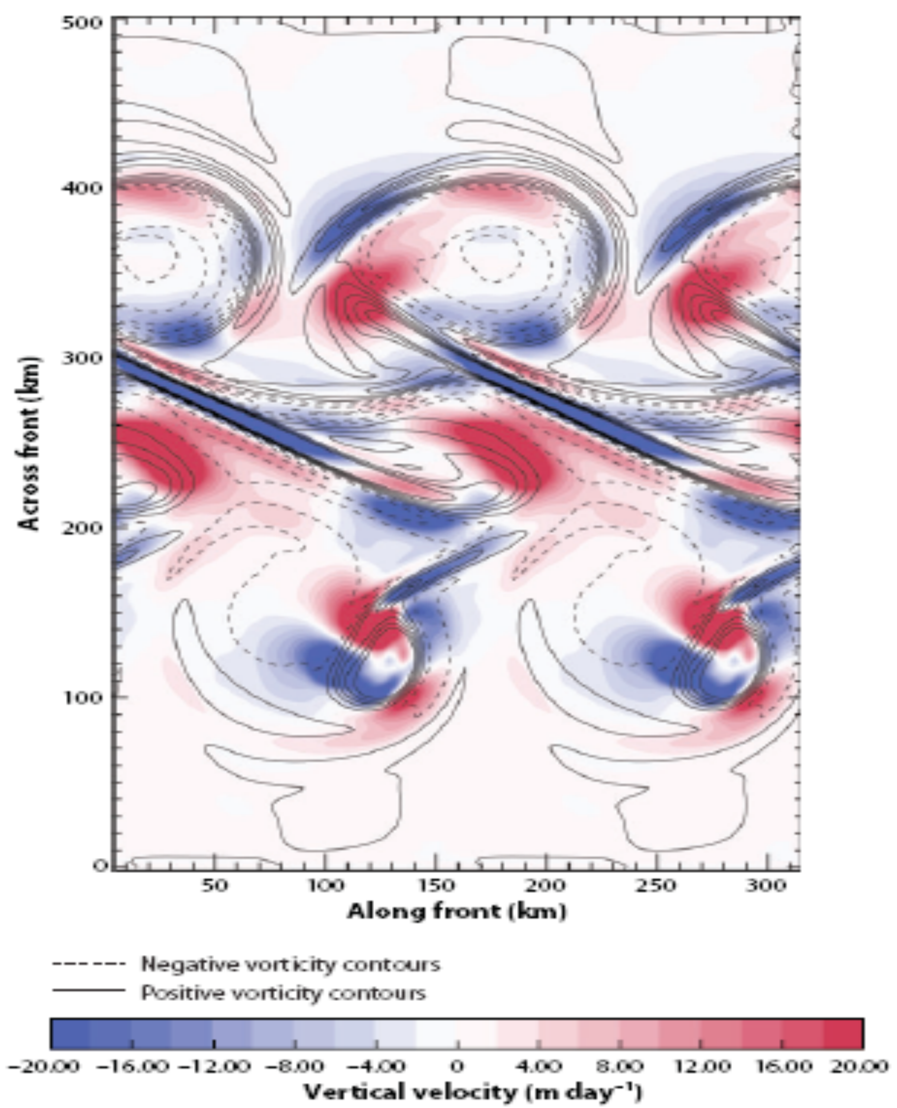

Vertical velocities at 90 m (*red for upward and blue for downward*).

Vorticity Field, ζ/f

Koszalka et al, JGR 2009

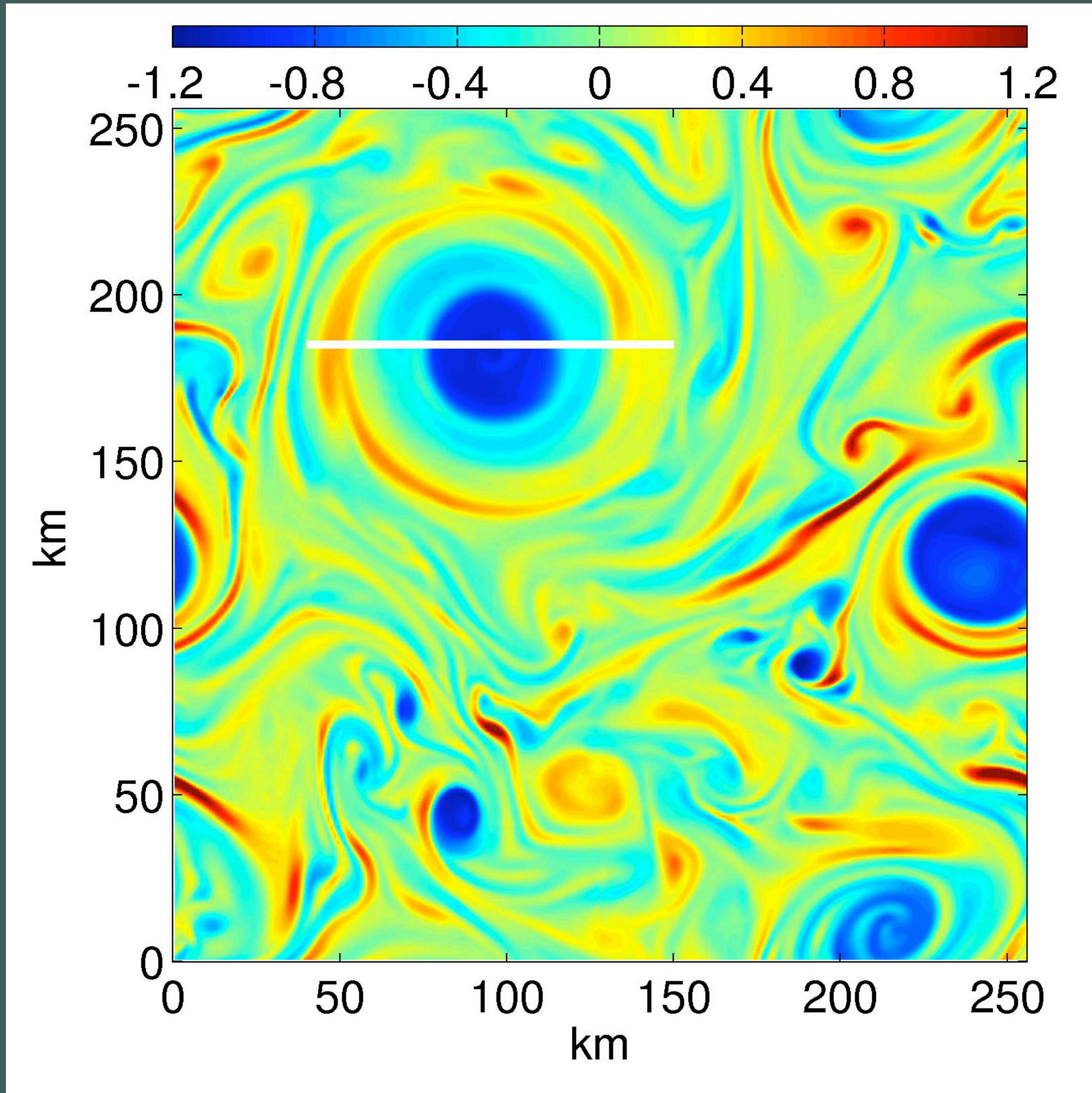

How does the vertical velocity field associated with a vortex look like?

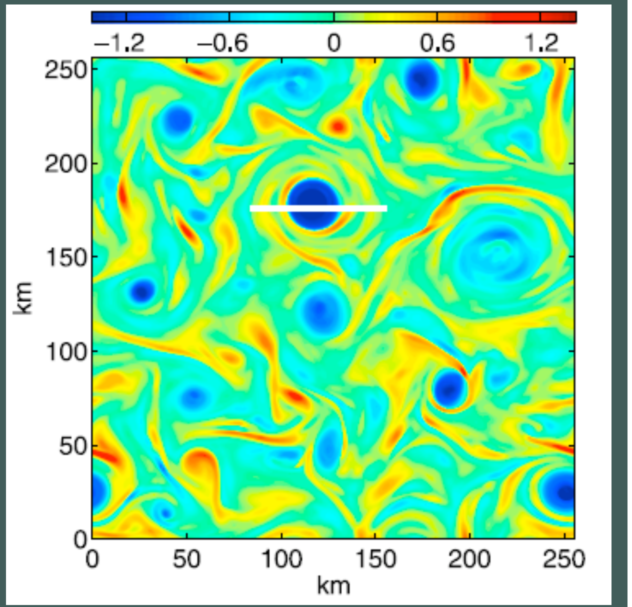

Daily averaged

Vertical Section	horizontal section at 78m	and at 350m (m/day)

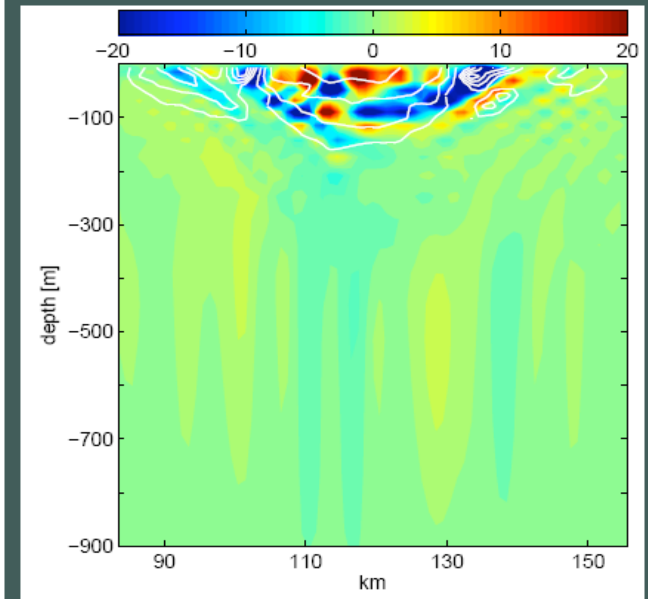

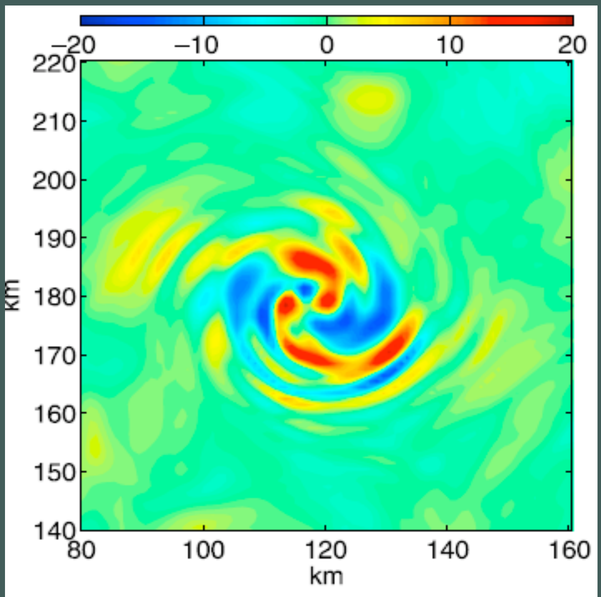

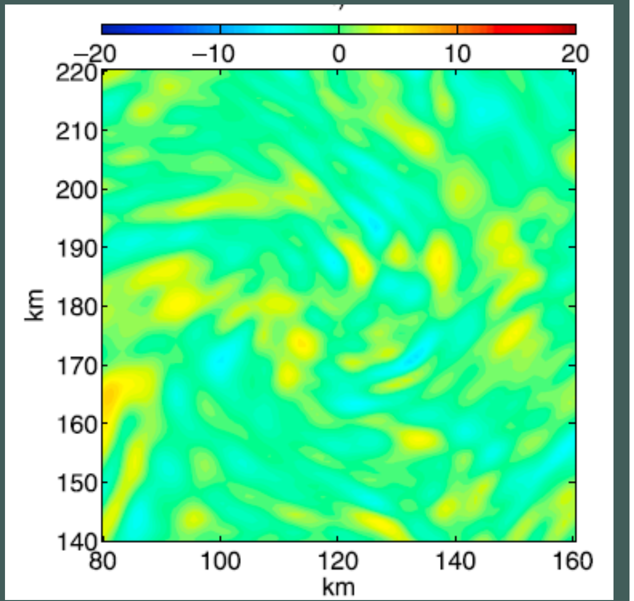

Looks even more complicated if we do not average over one day…

Vortex Rossby waves
VRW

again 78 and 350m, in m/day

near-inertial oscillations
NOI

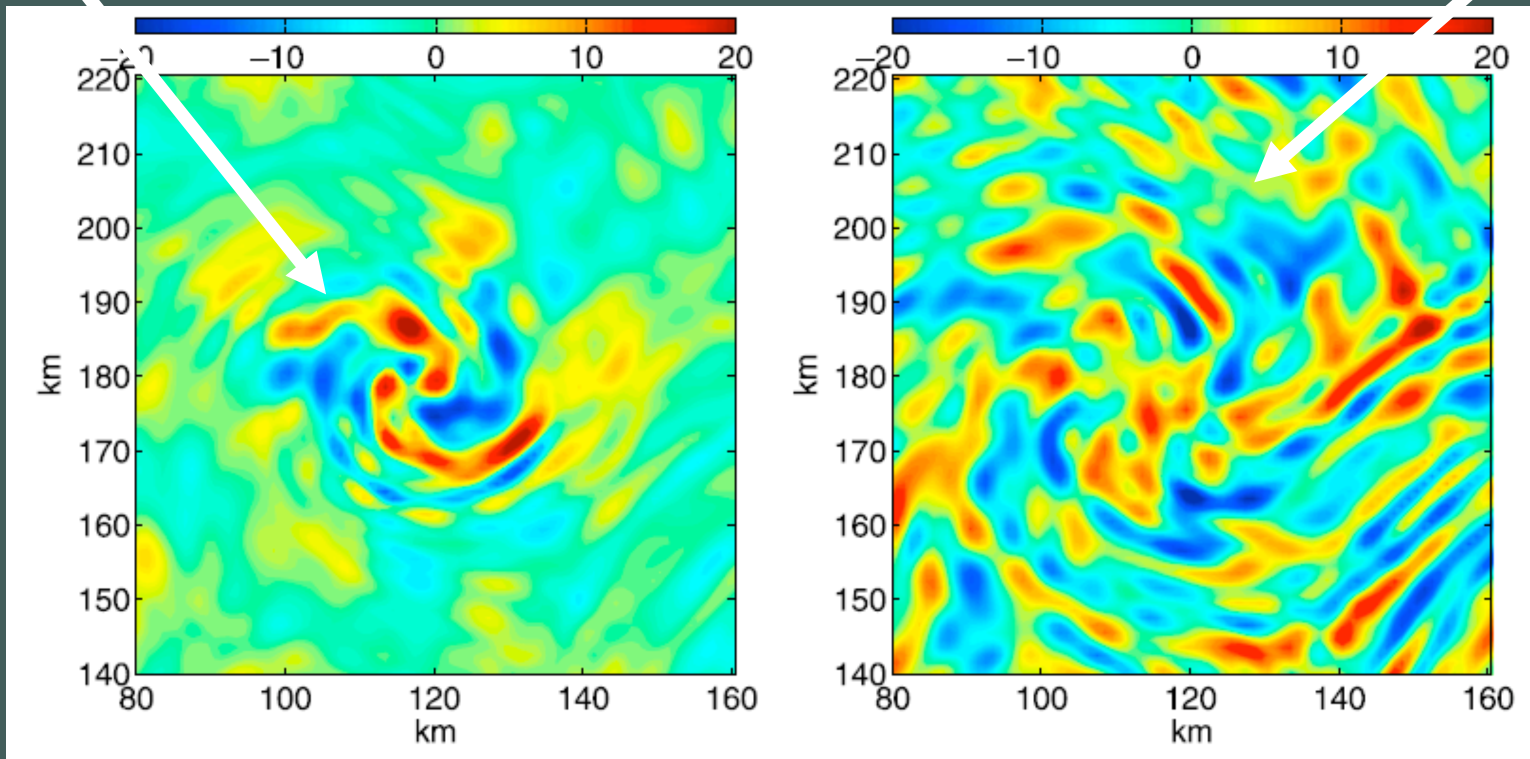

with primitive equations (ROMS)

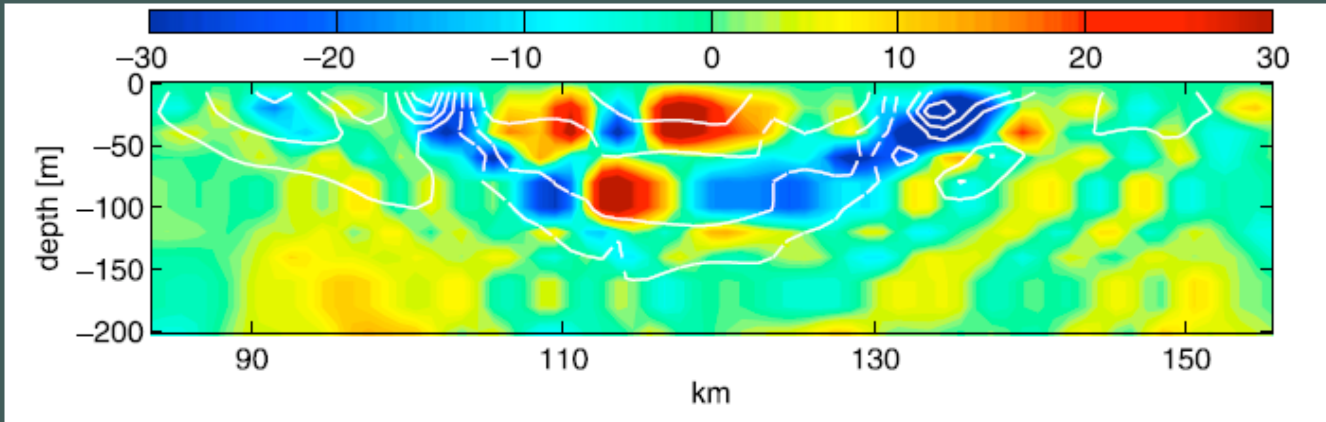

with the omega-equation

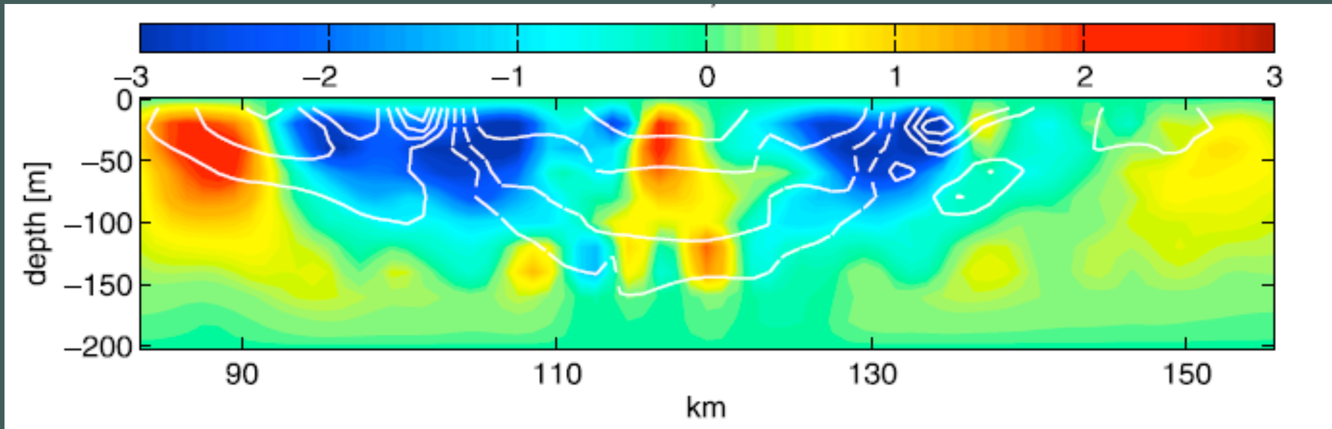

as a result vertical velocities strongly impact the vertical displacement of passive tracers

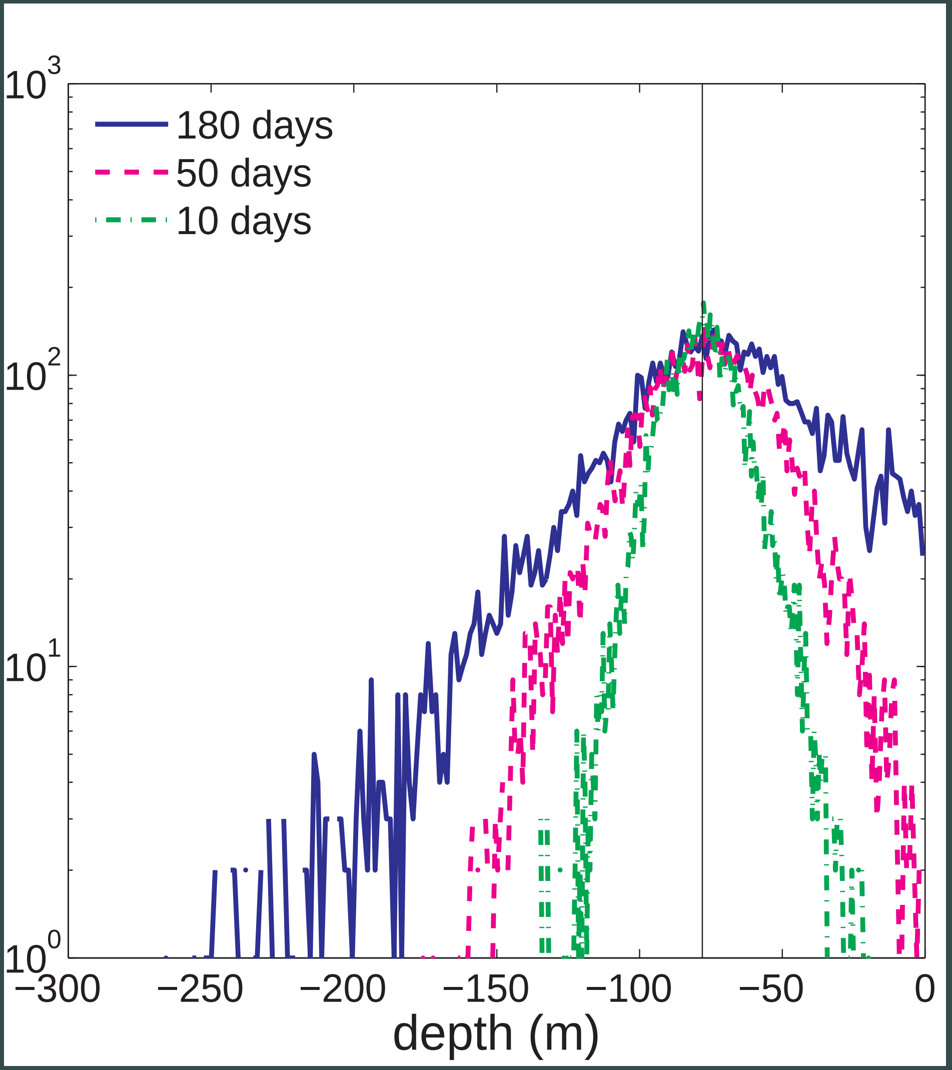

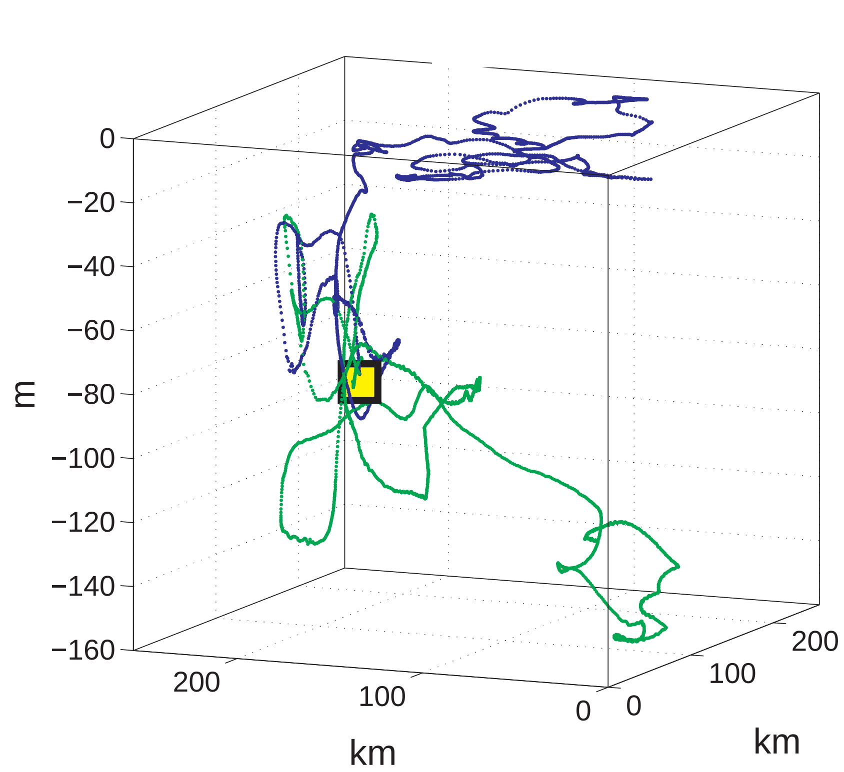

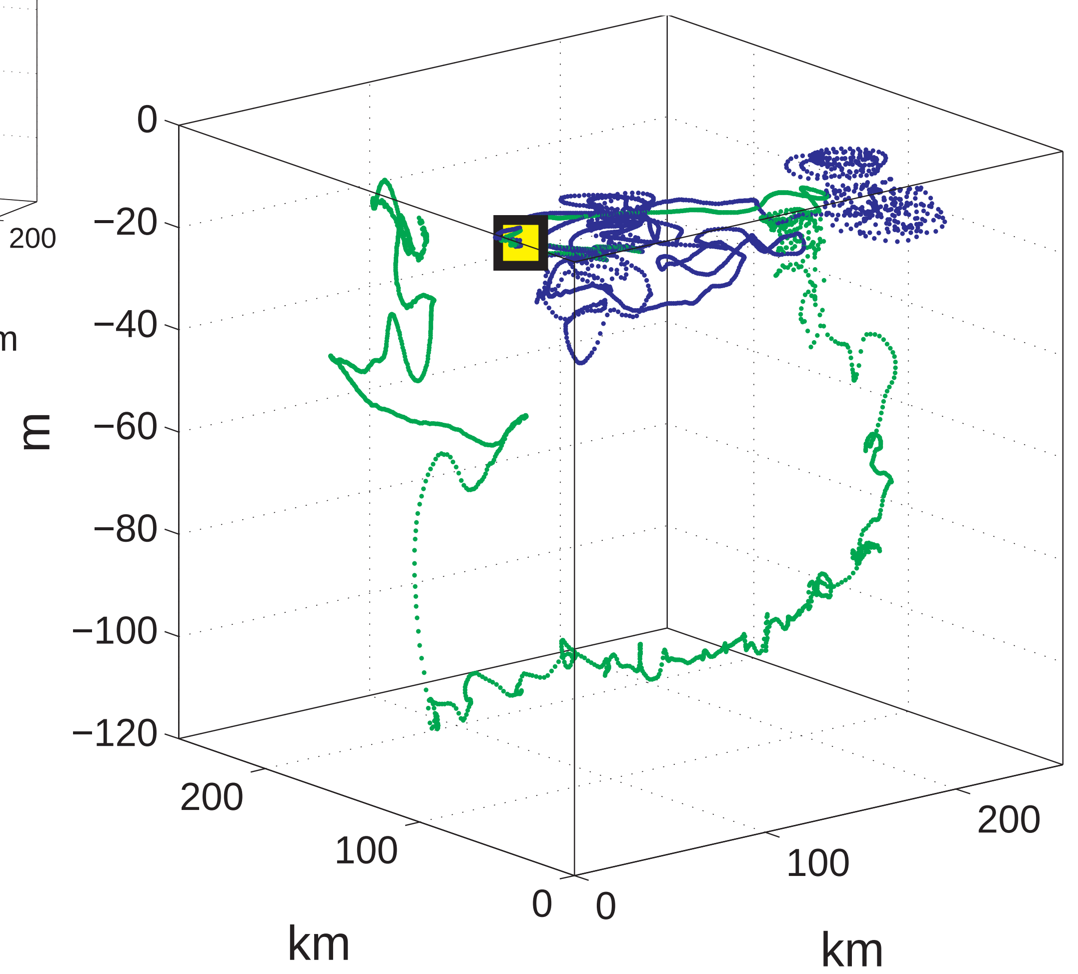

Example trajectories of initially close-by particle pairs released at 78m (top) and at the surface (right)

conclusions

- NIOs and VRWs associated with submesoscale unbalances motions in fronts and vortices represent an important mechanism for diapycnal mixing in the ocean. Their contribution has not been quantified yet.
- High frequency winds are indispensable for ocean models. Likely needed every 3 hours
- We do not know how the submesoscale physics interact with the biology. We can only say that the traditional (balanced) picture is far from complete/correct